MASTER OF SCIENCE (1977)
(Physics)

McMaster University
Hamilton, Ontario

TITLE: Spin and Parity Assignments in ^{63}Zn

AUTHOR: Peter Aish Seymour Metford, B.Sc.
(University of Western Ontario)

SUPERVISOR. Professor John A. Cameron

NUMBER OF PAGES. vii,43

SPIN AND PARITY ASSIGNMENTS IN ^{63}Zn

By

Peter Aish Seymour Metford, B.Sc.

A Thesis

Submitted to the School of Graduate Studies

in Partial Fulfilment of the Requirements

For the Degree

Master of Science

McMaster University

November 1977

ABSTRACT:

The two reactions, $^{60}Ni(\alpha,n\gamma)^{63}Zn$ (E_α = 12.0 Mev) and $^{64}Zn(p,d)^{63}Zn$ (E_p = 18.0 Mev) were studied.

γ angular distributions and γ-γ coincidence yields were extracted and correlated to ascertain the ^{63}Zn decay scheme. ℓ values and spectroscopic factors were determined from DWBA fits to the neutron pickup cross sections. The following spin and parity assignments were made to the low-lying states of ^{63}Zn: E=626.5 kev ($J^\pi=1/2^-,3/2^-,5/2^-$), E=637.0 kev ($J^\pi=7/2^-$), E=650.0 kev ($J^\pi=5/2^-$), E=1023.2 kev ($J^\pi=3/2^-$), E=1206.4 kev ($J^\pi=7/2^-$), E=1284.8 kev (J =5/2), E=1436.7 kev (J =3/2,5/2), E=1703.8 kev (J =7/2), E=1861.6 kev (J=7/2). E=2050.8 kev (J =9/2). A level at 1392.4 kev was observed in the (p,d) experiment. The state at 1063.9 kev was observed to be a doublet, with a separation of less than 1.5 kev ($J^\pi=7/2^-$, $J^\pi=(1/2^-)$).

Acknowledgements

I would first of all like to acknowledge John Cameron's immense cheerfulness, enthusiasm and expertise in helping me to do the research for this thesis. I would also like to thank Terry Taylor for his help in performing the experiments.

Much appreciation is also due Arif Khan for his useful unofficial advise.

Without the help of the Operations staff of the McMaster Accelerator Lab. ; in particular John McKay, Jim Stark and Y Peng, this thesis obviously would not have been possible.

Last, but definitely not least , is the support and encouragement given to me by my wife. In fact this thesis is dedicated -----

TO AGGIE

Table of Contents

List of Figures

List of Tables

Introduction

The nucleus $^{63}_{30}Zn_{33}$ may be described in terms of the shell model with 2 protons and 5 neutrons in the fp shell. An analysis of the properties of the low-lying states in the ^{63}Zn spectrum would provide a good test of the shell model in this mass region. In particular, an exhaustive study of the zinc isotopes using parameters fitted to the well-known copper and nickel isotopes has made detailed predictions regarding this nucleus (van Hienen et al 1976). However little data has been available for comparison.

To assist the reader in familiarising himself with the ^{63}Zn nucleus, the Nuclear Data Sheets summarizing the experimental state of the art and the adopted level scheme have been attached (fig.1).

The spins and parities of the ground state and the first two excited states at 193 and 248 kev have been confirmed as $3/2^-$, $5/2^-$ and $1/2^-$ respectively (Geisler 1971, Brandan and Haeberli 1977). However the experimental evidence concerning higher levels in ^{63}Zn is ambiguous and often contradictory.

The triplet at 626 kev, 636 kev and 650 kev (Geisler 1971, Sawa 1971, Birstein et al 1967) has not been resolved in the particle experiments, but an ℓ value of 1 has been assigned to this triplet (Johnson and Jones 1968, Betigeri et al 1967). Giesler (1971) made tentative spin and parity assignments to the 636 kev and the 650 kev levels of $1/2^-$ and $3/2^-$ respectively, based on ^{63}Ga β^+ decay experiments.

The suggestion that a doublet is at 1040 kev was made by the $^{64}Zn(p,d)^{63}Zn$ and the $^{64}Zn(^3He,^4He)^{63}Zn$ single-neutron transfer experiments (Johnson and Jones 1968, Betigeri et al 1967) since the differential

cross section angular distributions were fitted by an $\ell = 1+3$ mixture. The analysis of $^{63}Cu(p,n)^{63}Zn$ neutron time-of-flight experiments (Tanaka et al 1970) resolved this doublet, placing the two levels at 1028±5 kev and 1070±5 kev.

Most of the energy levels assigned to the ^{63}Zn spectrum above the 1060 kev state were determined by a decay scheme from the $^{60}Ni(\alpha,n\gamma)^{63}Zn$ experiment (Sawa 1971) and the neutron time-of-flight experiment (Tanaka et al 1970). However there are contradictions, eg. Tanaka (1970), assigns two levels at 1403 kev and 1444 kev while Sawa (1971) places only one level at 1436 kev.

Hence we can see that there is a need for clarification of the ^{63}Zn spectrum.

The two reactions $^{60}Ni(\alpha,n\gamma)^{63}Zn$ and $^{64}Zn(p,d)^{63}Zn$ were studied. γ angular distribution and γ-γ coincidence data were obtained and correlated yielding information on the ^{63}Zn decay scheme. Energy levels, relative ℓ values and spectroscopic factors were extracted from the neutron pick-up experiments. These two experiments were then compared, producing a fairly complete picture of the low-energy ^{63}Zn spectrum.

Chapter I

The $(\alpha, n\gamma)$ Reaction

I.1 Theory

In order to extract nuclear spins and multipole mixing ratios the gamma angular distribution is necessary. It may be shown (Rose and Brink 1967) that the anisotropy of the angular distribution is related to the degree of alignment of the initial state from which the γ transition occurred. A nuclear state of spin J is said to be aligned if the magnetic substate population $P_J(m) = P_J(-m)$ where $0, 1/2 \leq m \leq J$ and the Oz axis is chosen to be in the direction of the incident beam. Although these population parameters are in principle calculable using various theories, generally it is assumed that they have a gaussian distribution of the form (Sawa 1973):

$$P_J(m) = \frac{\exp(-m^2\sigma^2/2)}{\sum_{m_i=-J}^{J} \exp(-m_i^2/2)}$$

In a series of experiments using alpha-induced reactions on spin-zero targets in the fp shell (Sawa 1973) it was found that a surprisingly high degree of alignment ($\sigma = 1.5$) was obtained. This was thought to be due to the small amount of orbital angular momentum ($\ell = 0, 1$) carried out of the compound nucleus by the neutron (fig. 2).

The analysis of a γ of multipolarity L, L' produced by the transition from a state of spin J_i to a state of spin J_f yields a general expression for the the angular distribution of the form (Rose and Brink 1967) :

$$W(\theta) = 1 + A_2 P_2(\cos\theta) + A_4 P_4(\cos\theta)$$

where $P_k(\cos\theta)$ is the k^{th} Legendre polynomial.

$$A_k = B_k(J_i)\, Q_k \left(R_k(LLJ_iJ_f) + 2\delta R_k(LL'J_iJ_f) + \delta^2 R_k(L'L'J_iJ_f) \right)/(1+\delta^2)$$

the B_k coefficient describes the nuclear alignment:

$$B_k(J_i) = \sum_{m_i=-J_i}^{J_i} P(m_i)(-)^{(J_i-m_i)}(2J_i+1)^{\frac{1}{2}}\, (J_iJ_im_i-m_i|k0)$$

and $P(m_i)$ is the population of the m^{th} magnetic substate. The Q_k coefficient is the solid-angle attenuation coefficient of the detector.

$$R_k(LL'J_iJ_f) = (-)^{(1+J_i-J_f+L'-L-k)} \left((2J_i+1)(2L+1)(2L'+1) \right)^{\frac{1}{2}} (LL'1-1|k0)\, W(J_iJ_iLL';kJ_f)$$

and the mixing ratio δ is defined as the ratio of the reduced matrix elements of the two multipoles L, L' :

$$\delta = \frac{\langle J_i \| T_L \| J_f \rangle}{\langle J_i \| T_{L'} \| J_f \rangle} \left((2L'+1)/(2L+1)\right)^{\frac{1}{2}}$$

where T_L is the interaction operator between the γ-and the nucleus (Rose and Brink 1967).

I.2 The $^{60}Ni(\alpha,n\gamma)^{63}Zn$ Reaction

I.2a Target Preparation

The ^{60}Ni target was rolled to a thickness of approximately 0.5 mm and mounted on a backing of 0.015 in. thick tantalum. This target assembly was then glued to a 0.125 in. thick aluminum support which threaded into the bottom of the target chamber and positioned at an angle of 45° to the incident alpha beam (fig. 3).

I.2b Angular Distribution Measurements

To obtain an angular distribution, a 50cc Ge(Li) detector was

placed on a movable mount which rotated about the axis of the target chamber. The Ge(Li) was a distance of 10 cm from the target, yielding attenuation factors of $Q_2 = 0.98$ and $Q_4 = 0.94$ (Camp and Van Lehn 1969). X-ray and low energy γ yields were reduced by using a 1 mm thick lead absorber in front of the detector. The 12 Mev alpha beam was obtained from the McMaster FN Tandem van de Graaff accelerator.

The yields at the 5 angles $0^\circ, 35^\circ, 55^\circ, 70^\circ, 90^\circ$ were collected for approximately three hours per angle using the on-line PDP-9 computer (fig.4). The spectra were internally calibrated using the well-known strong 365.0, 669.6, 962.1 and 1327.0 kev gamma transitions in ^{63}Cu (Nuclear Data Sheets 1975, drawing 7) which was produced by the competing reaction $^{60}Ni(\alpha,p\gamma)^{63}Cu$. Peak energies and areas were extracted using the program SOFT on the PDP-15 computer. The energy resolution was 1.6 kev FWHM. Errors for the ^{63}Zn γ transition energies were calculated using the same program and were statistical.

The peak areas were corrected for absorption effects which were asymmetric with respect to angle (Davisson and Evans 1952) and then normalised to the isotropic gamma angular distribution from the $J^\pi = 1/2^-$ 248.4 kev transition in ^{63}Zn (Giesler 1971, Brandan and Haeberli 1977).

To construct an efficiency curve the experimental yields of the 365.0 kev and the 1327.0 kev branches from the 1327.0 kev level in ^{63}Cu were corrected for absorption effects and compared to the branching ratios obtained by the experiment $^{63}Cu(p,p\gamma)^{63}Cu$ (Nuclear Data Sheets 1975, drawing 6). Using this efficiency curve relative γ intensities were calculated (fig.5).

A_2 and A_4 coefficients were obtained as a function of assigned initial and final spins, the mixing ratio δ and the population

parameters of the initial state. The goodness of fit was determined by minimising χ^2 as a function of δ where $-90^\circ \leq \tan^{-1}(\delta) \leq +90^\circ$. It was assumed that the population parameters had a gaussian distribution with $\sigma = 1.0$. The value for σ was obtained by fitting the angular distributions of the 1206.4 kev and the 192.9 kev transitions over a range of σ ($0.5 \leq \sigma \leq 3.0$). The 1206.4 kev transition was chosen since it had a characteristic stretched E2 angular distribution , and characteristics of the 192.9 kev transition have been previously measured (Nir and Cameron 1977, Birstein et al 1968) (fig 6).

I.2c γ-γ Coincidence Measurements

In this experiment two 50cc Ge(Li) detectors were fixed with respect to each other and to the alpha beam. To assist in minimising intercrystal scattering, the Ge(Li)s were not facing each other and heavy lead shielding was placed on the beam line between them . 1mm thick lead absorbers were placed on the front of the detectors to reduce x-rays and low energy γ yields.

The coincidence circuit (fig .7) selects pairs of events which occur within the time resolution of the experiment which was 8.3ns FWHM. The advantage of this circuit is that it selects as true coincidences only those events which form cascading transitions within the residual nucleus. The three parameters time, energy and energy were fed into the PDP-9 computer which was programmed to address record these data on magnetic tape using the program AR3P. Ten 1500 foot magtapes were collected, each containing approximately 1.4 million coincidence events.

To analyse these data, projections were taken of the coincidence

spectrum of the first Ge(Li) and of the TAC time spectrum. Gates were set on the peaks of interest in the Ge(Li) projection and on the desired time resolution and input into the PDP-15 sorting program MS3PJJ along with the appropriate backgrounds. The data were then sorted, contracted by a factor of 2 and plotted (fig.8).

A list of the gates and the peaks seen in each is given in table 1. ^{63}Cu contamination was seen in some of the gates whose energies were similar to transitions in the ^{63}Cu decay scheme.

The presence of ^{63}Cu lines in the 413 kev gate was explained when the 413 kev line was seen in the ^{63}Cu 962 kev and 1130 kev gates and placed between the 2093 kev and the 2504 kev levels in the ^{63}Cu decay scheme (Nuclear Data Sheets 1975, drawing 8).

In several of the gates high energy lines were seen but not placed in the decay scheme. A list of these unplaced lines is also given in table 1.

The 636 kev gate overlapped slightly on the 640 kev line which explains the presence of the 413 kev line, however the 1057 kev line possibly indicates that there is a level at 1691 kev. A peak corresponding to this energy was seen in the ^{60}Ni(α,nγ)^{63}Zn singles spectra, but there is no other evidence for its existence, although Geisler(1971) reported a level at this energy.

In a similar vein, the 767 kev gate was examined to check the existence of a level at 1392 kev, however all of the lines seen in the gate may be explained in terms of the 765.8 kev transition in ^{63}Cu (Klaase and Goudsmit 1974).

The decay scheme is shown in fig.9

I.2d Experimental Analysis

Simultaneously using the results of the angular distribution measurements and the decay scheme developed by the $\gamma-\gamma$ coincidence data spin assignments were made. The spins of the first three levels were assumed to be $3/2^-$, $5/2^-$ and $1/2^-$ respectively.

The 626.5 kev level

The 626.5 kev transition to the $3/2^-$ ground state appeared to have an isotropic distribution. Hence we could only say that its spin was not 7/2, however the spin could equally be any of 1/2, 3/2 or 5/2. (J=1/2,3/2,5/2)

The 636.0 kev level

The 636.0 kev transition had a characteristic stretched E2 angular distribution. This level was assigned a spin and parity $7/2^-$. ($J^\pi = 7/2^-$)

The 650.0 kev level

The 650.0 kev transition had a best fit for an initial spin of 5/2 and this was confirmed by the 650.0 kev - 192.9 kev transition. (J=5/2)

The 1023.2 kev level

The 1023.2 kev transition was fitted well for spins of 3/2 or 5/2. The 1023.2 kev - 650.0 kev transition did not disprove either of the two possibilities, but the 1023.2 kev - 248.4 kev transition could not be fitted with an initial spin of 5/2, and did have an acceptable χ^2 for the 3/2 spin choice. (J=3/2)

The 1063.9 kev level

The 1063.9 kev transition had an E2 distribution and was assigned an initial spin and parity of $7/2^-$. The imperfect fit was attributed to an inappropriate choice of σ. The 1063.9 kev - 192.9 kev transition had an acceptable

fit only for an initial spin of 7/2 while the 1063.9 kev - 650.0 kev transition was ambiguous. ($J = 7/2^-$)

The 1206.4 kev level

An initial spin and parity of $7/2^-$ was assigned based on the 1206.4 kev transition's characteristic E2 angular distribution. ($J = 7/2^-$)

The 1284.9 kev level

The best fit for the 1284.9 kev was obtained for an initial spin of 5/2. This was confirmed by the 1284.9 kev - 248.4 kev branch. The 1284.9 kev - 192.9 kev transition was fitted equally well for initial spin choices of 5/2 or 7/2 . (J=5/2)

The 1392.4 kev level

No data were available for analysis since the 1392.4 kev transition is too weak, and the other branch that was assigned to it (Giesler 1971) is masked by the 2092.7 kev - 1327.0 kev transition in ^{63}Cu (Klaase and Goudsmit 1971).

The 1436.7 kev level

The ground state transition of the level was fitted equally well with an initial spin of either 3/2 or 5/2 . The other branch, the 1244.3 kev transition to the $5/2^-$ 192.9 level had a stretched E2 distribution, but as previously mentioned, the 2208.0 kev - 962.0 kev transition in the ^{63}Cu spectrum has a similar energy. A fit was attempted with an initial spin of 9/2 for the 1436.9 kev transition which had negative results. (J=3/2,5/2)

The 1691 kev level

No data were available for analysis.

The 1703.8 kev level

The 1703.8 kev - 1063.9 kev transition had an acceptable fit for an initial spin of either 5/2 or 9/2 . The other branch to the 1206.4 kev level again suggested these spins. However the 5/2 spin choice seems improbable since this state is only observed to decay to spin 7/2 levels and not to those of lower spin. (J = 7/2)

The 1861.6 kev level

An initial spin of 7/2 yielded the best fit for the 1861.6 kev - 1063.9 kev branch while the 1861.6 kev - 650.0 kev transition did not have a good fit for any of the possible spin choices. (J=7/2)

The 2050.8 kev level

The 2050.8 kev - 1063.9 kev transition had a best fit for an initial spin choice of 9/2 . (J=9/2)

The 2585.2 kev level

No analysis was fruitful since the 881.4 kev transition is to close to the 881 kev transition from the 2208 kev level to the 1327.0 kev level in ^{63}Cu.

These results are summarized in table 2. Some of the angular distributions are shown in fig.10.

Chapter II

The (p,d) Reaction

II.1 Theory

The single neutron pickup experiment $^{64}Zn(p,d)^{63}Zn$ was analyzed using direct reaction theory. In this model it is assumed that the reaction is a one-step process taking place on a very fast time scale (10^{-22} sec). The incident proton picks up a target neutron forming the residual nucleus ^{63}Zn in some excited state and a deuteron without the formation of an intermediate compound state. Since the ^{64}Zn ground state has spin and parity $J^{\pi} = 0^{+}$, the spin of the ^{63}Zn residual nucleus $j = \ell \pm \frac{1}{2}$ with parity $(-)^{\ell}$ where ℓ is the orbital angular momentum of the transferred neutron relative to the ^{63}Zn nucleus. The quantity ℓ is usually determined from a description of the ^{63}Zn nucleus in terms of the shell model.

Assuming an inert ^{58}Ni core , the ^{64}Zn ground state may be described by assuming that the two protons couple to $J^{\pi} = 0^{+}$ and the six neutrons occupy the $2p_{3/2}$, $1f_{5/2}$ and the $2p_{1/2}$ orbitals. However there is evidence (van Hienen et al 1976) that the $1g_{9/2}$ shell also plays a role in the description of higher lying levels in the odd-mass zinc isotopes.

It has been empirically observed that the angular position of the strong forward peak in the differential cross section angular distribution is strongly dependent on the value of ℓ . In actual practice ℓ is determined

by comparing the experimental cross section angular distribution with the predictions made by the distorted wave Born approximation (DWBA) direct reaction theory (Austern 1970).

II.1a The Distorted Wave Born Approximation

The DWBA makes the assumption of several models. To calculate the DWBA differential cross sections one requires the elastic scattering wave functions of the incident and outgoing particles since the overlap of these wave functions determines the probability of finding the incident and outgoing particles near the nucleus where the neutron transfer takes place. The elastic wave functions are calculated from a knowledge of the optical potential model for the nucleus in question. The optical model that was used has the form:

$$V(r) = -V_R f(r,r_R,a_R) - iW_V f(r,r_V,a_V) + 4a_s i \frac{d}{dr} W_s f(r,r_s,a_s) + V_{so} \frac{2}{r} \frac{d}{dr} f(r,r_{so},a_{so}) \underline{S}\cdot\underline{L} + V_{coulomb}$$

where the Woods-Saxon function $f(r,r_i,a_i) = (1+\exp(r-r_i A^{1/3})/a_i)^{-1}$

The imaginary terms determine how much of the elastic wave function is "damped" by loss of elastic particles due to inelastic events and the first derivative of the Woods-Saxon potential indicates a surface effect. Provision is also usually made for non-local potentials in the form of a mass-dependence of the coefficients. The optical model parameters are determined by making a fit of this potential to the appropriate scattering data.

It is also assumed that the target nucleus ^{64}Zn may be described

as a neutron coupled to the ^{63}Zn residual nucleus with the neutron in some shell model state. Hence DWBA calculates the differential cross sections on the basis that the energy levels in ^{63}Zn are single particle shell model states. The ratio between the experimental and the DWBA differential cross sections is called the spectroscopic factor S. Thus if the wave function of the final state can be completely described as a neutron hole pure shell state, S=1. However if the energy level of interest is only partly composed of a single particle shell model state, S will be small.

II.2 The $^{64}Zn(p,d)^{63}Zn$ Reaction

II.2a Target Preparation

Since a thin self-supporting ^{64}Zn target will sublimate if an 18 Mev proton beam is fired at it, a Carbon-Zinc-Carbon sandwich target was used.

A glass slide was obtained with a $10\mu gm/cm^2$ layer of carbon coated on one side. Zinc oxide with a ^{64}Zn isotopic purity > 99.99% was reduced by mixing with carbon and heating in a tungsten crucible. An approximately $100\mu gm/cm^2$ thick layer of ^{64}Zn was deposited on the slide during the reduction heating process. A second layer of $10\mu gm/cm^2$ thick carbon was then evaporated onto the zinc. Finally this sandwich was floated off the glass in water and placed on an aluminum frame.

II.2b Cross Section Measurements

The 18 Mev proton beam was obtained from the McMaster FN Tandem van de Graaff accelerator.(1) The beam was stopped in an electron suppressed

(1) Initially the reaction $^{64}Zn(d,t)^{63}Zn$ was tried, however it proved impossible to resolve the elastic deuterons from the tritons.

faraday cup. The reaction products were momentum-analyzed in an Enge split-pole spectrograph (Spencer and Enge 1966)

Spectra were obtained using a resistive wire proportional counter. This detector had two resistive wires separated by a thin aluminum foil. Particle position and energy loss information was obtained from the front counter and the back counter was again used for ΔE information. This redundancy of information was necessary since the large negative Q-value (-9.630 Mev) for the (p,d) reaction produced deuterons with approximately the same magnetic rigidity as the elastic protons. Hence it was necessary to select the deuterons from the appallingly large background of elastic events using energy-loss techniques. Most of the protons were cut out by appropriately setting the baseline window of the TSCA on the signal from the back counter (fig.11).

The spectra were displayed using the on-line PDP-9 computer , which via software logic calculated the position and energy loss spectra from the front counter. Windows were set on the deuteron group in the ΔE spectrum (fig.12) and the deuteron position spectrum was obtained (fig.13).

Biases of 1100 V and 1000 V were applied to the front and back counters respectively through the pre-amps. A slow flow of a gas mixture of 90% Argon and 10% Methane was used at a pressure of 700 mmHg .

An incident proton beam of approximately 40 namps was used. This figure was reduced at the forward angles to minimize dead-time effects.

The magnetic fields and kinematic shifts for the reactions of interest were calculated by the program MAGGIE.

Peak areas were extracted using the program SOFT. Position resolution was 6.4 channels FWHM or 1.28 mm .The dispersion was 20 kev/mm.

Hence the triplet at 628 kev was not resolved.

Relative differential cross sections were calculated by normalising the peak areas to the dead-time corrected digital output from the faraday cup. To determine the absolute cross sections, another experiment was performed where the yields of both the $^{64}Zn(p,d)^{63}Zn$ ground-state deuterons and the $^{64}Zn(p,p)^{64}Zn$ elastic protons were extracted at the lab angle 30°. Relative cross sections were again calculated using the above method. The relative elastic cross section was then compared to the DWBA elastic cross section at 30° . This ratio was then used to determine the absolute differential cross section for the ground state at 30°, enabling absolute cross sections to be determined for the previous experiment.

II.2c Experimental Analysis

A total of nine levels were resolved in the low-energy ^{63}Zn spectrum. Optical model parameters for the protons and the deuterons were calculated from the empirical results of Becchetti and Greenlees (1969) and from Lohr and Haeberli (1974) (table 3). The neutron well depth was adjusted to fit the ^{64}Zn neutron separation energy. A Thomas spin-orbit potential was also included in the neutron potential.

DWBA cross sections were calculated using the CDC6400 computer code DWUCK (Kunz 1974). Fits to the angular distributions of the five states of energy 000.0 kev, 192.9 kev, 248.4 kev, 1023.2 kev, and 1206.4 kev yielded ℓ values and spectroscopic factors (fig14). The assigned ℓ values for the ground state and first two excited states agreed with previous experimental results (Johnson and Jones 1968, Brandan and Haeberli 1977).

The spectroscopic factors are larger than those calculated by Brandan and Haeberli (1977), however the ground state value agrees with Johnson and Jones (1963) and Betigeri et al (1967).

The three states of energies 1284.8 kev , 1392.4 kev and 1436.7 kev were not fitted (fig15).

The 1063.9 kev level had an anomalous angular distribution indicating an ℓ=1+3 mixture. This suggested that there is either an unresolved doublet at this energy or that some form of compound reaction mechanism populates this state (fig.14).

The unresolved triplet at 629 kev was found to have a predominantly ℓ=1 angular distribution (fig.14). A gaussian fit to the peak at 30° with fixed energies of 627 kev, 637 kev and 650 kev and the FWHM = 6.4 channels yielded relative intensities of 74%, 20% and 6% respectively. Hence the 627 kev state was assigned ℓ=1. The other states were assigned ℓ=1 or 3.

Chapter III

Comparison of Experiments

The spins and parities of the ground state and the first two excited states agreed with the accepted values (Nuclear Data Sheets 1975, drawing 10, Brandan and Haeberli 1977).

The 626.5 kev level

The $\ell=1$ assignment to this state agreed with the $(\alpha,n\gamma)$ experiment which fitted initial spins of 1/2, 3/2 or 5/2 to the 626.5 kev transition. $(J = 1/2^-, 3/2^-)$

The 637.0 kev level

The tentative assignment of an initial spin of 7/2 to the 637.0 kev transition agreed with the proposal that this state has either an $\ell=1$ or 3 distribution. However the question as to why a branch to the $5/2^-$ 192.9 kev state is not seen in the decay scheme does not have an answer. $(J=(7/2^-))$

The 650.0 kev level

This level was unambiguously assigned a spin of 5/2 from the $(\alpha,n\gamma)$ analysis. The DWBA analysis of the triplet indicated $\ell=1$ or 3. $(J=5/2^-)$

The 1023.2 kev level

The 1023.2 kev level was assigned a spin of 3/2 and $\ell=1$. $(J=3/2^-)$

The 1063.9 kev level

The anomalous behavior of this level can be explained in terms of a very closely-spaced doublet

The results of the (p,d) experiment suggested this hypothesis. since the differential cross section angular distribution was fitted with an $\ell=1+3$ mixture. It was also noted that the $7/2^-$ fit to the 1063.9 kev γ transition observed in the $(\alpha,n\gamma)$ experiment had a very bad fit.

If we assume that there is an isotropic component in this γ angular distribution, then the A_2 and A_4 coefficients will be reduced by a factor $(1-\alpha)$ where α is the strength of this isotropic component. The quantity α is determined by comparing the A_2 and A_4 coefficients calculated assuming a spin and parity $7/2^-$ to the empirical A_2 and A_4 coefficients fitted to the data using the program LEGPOL, and was found to have the value 0.50 ±.04. The fit to the 1063.9 kev γ transition angular distribution data , assuming an isotropic contribution of 50% is shown in fig.16 . ($J^\pi = 7/2^-$, $J^\pi = 1/2^-$).

Beyond this level the results of the (p,d)experiment were not fitted with DWBA, however states of energies 1284.8 kev, 1392.4 kev and 1436.7 kev were resolved. These levels agree with the ^{63}Zn decay scheme determined by the $(\alpha, n\gamma)$experiment. Hence the state at 1392.4 kev is only weakly populated by the $(\alpha, n\gamma)$reaction and its largest branch may be masked by the ^{63}Cu spectrum.

The 1691 kev level tentatively assigned to the ^{63}Zn spectrum was out of the proportional counter's energy range and so was not confirmed.

Although a $9/2^+$ state was expected to be in the ^{63}Zn spectrum in the region between 1 and 2 Mev (van Hienen et al 1976) , spin 9/2 states were identified at 1703.8 kev and 2050.8 kev from the analysis of the $(\alpha, n\gamma)$ experiment, no confirmation was available from the (p,d) experiment.

Chapter IV

Comparison with Theory

The modified surface delta interaction has been used to perform the shell model calculations for the zinc isotopes (van Hienen 1976). The surface delta interaction is based upon the following three assumptions:

(i) The residual interaction (which is that part of the interaction not included in the average one body shell model potential) only takes place at the surface of the nucleus.

(ii) The interaction only takes place if the nucleons are in the same place on the surface.

(iii) The interaction is independent of the orbital angular momentum of the nucleons.

Labelling the nucleons of interest i and j and if $\underline{r}_i$ is the position of the i^{th} nucleon

$$V_{ij} = -4\pi A_T \delta (r_i - R) \delta (r_j - R) \delta \Omega_{ij})$$

R is the nuclear radius and the interaction strength A_T is only dependent on the isospin of the coupled nucleons (Glaudemans et al 1967).

This interaction is modified by introducing a second term which again is only dependent on the isospin:

$$V_{ij} = -4 A_T \delta (r_i - R) \delta (r_j - R) \delta \Omega_{ij}) + B_T$$

In these calculations a ^{56}Ni inert core was assumed and the active particles are restricted to the $2p_{3/2}$, $1f_{5/2}$ and $2p_{1/2}$ shells. The MSDI parameters were fitted to the nickle and copper isotopes. A comparison of these calculations with the experimental results is shown in fig.16.

Chapter V

Suggestions for Future Experiments

The identity of the doublet centred at 1063.9 kev has not been confirmed. However it has been established that one of the components has a spin and parity $7/2^-$ and the other state was tentatively assigned a spin and parity $1/2^-$. Hence, by using different reaction mechanisms, it should be possible to confirm this low spin assignment. This could be done by performing both the $^{60}Ni(\alpha,n\gamma)^{63}Zn$ and the $^{54}Fe(^{12}C,p2n\gamma)^{63}Zn$ reactions using the same detector geometries. The heavy ion reaction preferentially populates the higher spin states since the ^{12}C beam brings in immense amounts of orbital angular momentum.

If the ^{12}C experiment were also performed in a γ-γ coincidence mode, it might be possible to assign some of the unplaced γ transitions seen in the $(\alpha,n\gamma)$ gates, since they presumably come from high-lying levels in the ^{63}Zn nucleus.

The ^{12}C ion beam experiment has been run, and the data are being analysed ar the present time.

fig.1

Nuclear Data Sheets summarising the "state of the art" of ^{63}Zn.

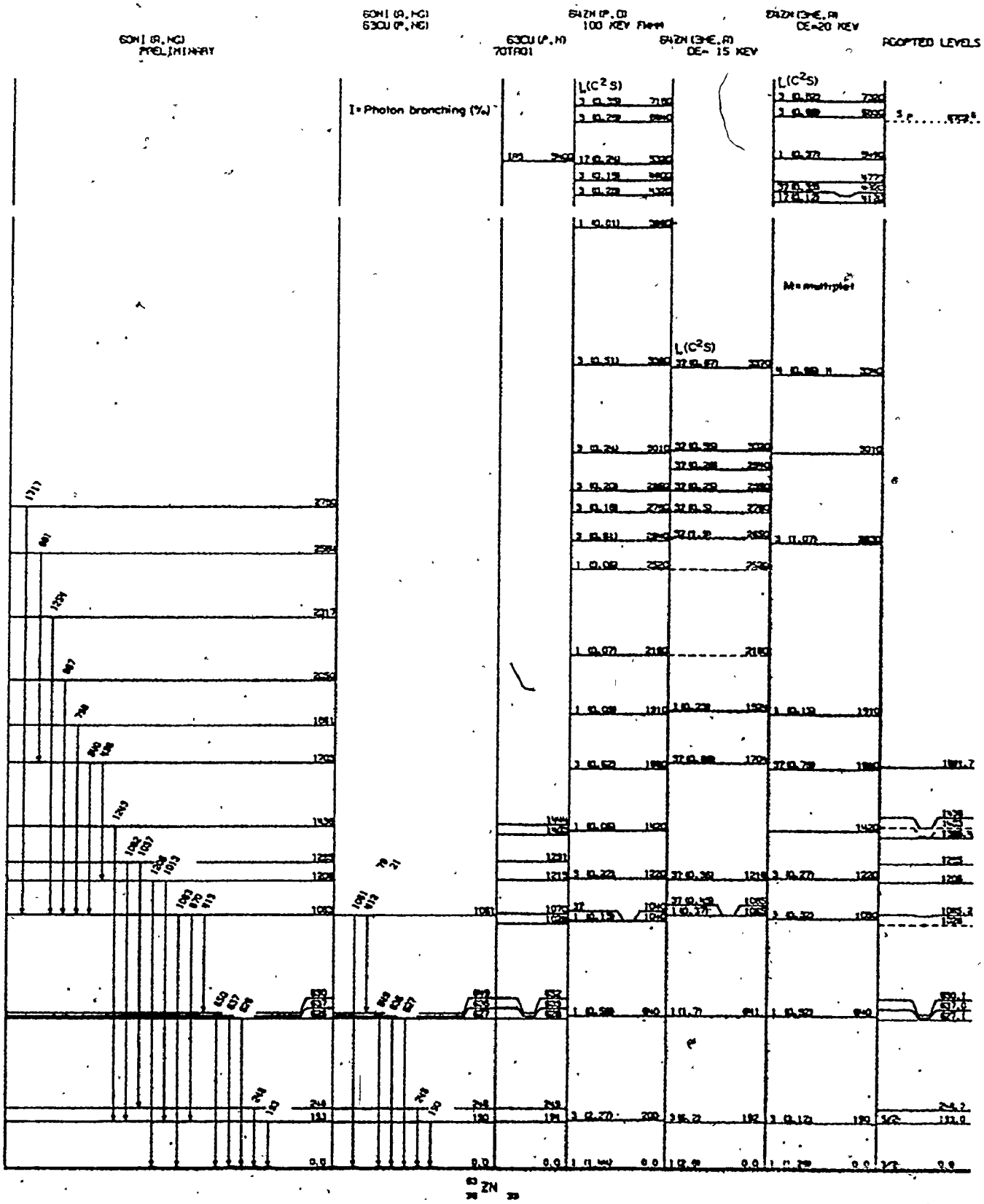
60NI (α,nG)
PRELIMINARY
60NI (α,nG)
63CU (p,nG)
63CU (p,t)
70TA01
64ZN (p,α)
100 KEV Plateau
64ZN (3He,α)
DE= 15 KEV
66ZN (3He,α)
DE=20 KEV
ADOPTED LEVELS
I = Photon branching (%)
M = multiplet
L(C2S)
63 30 ZN 33

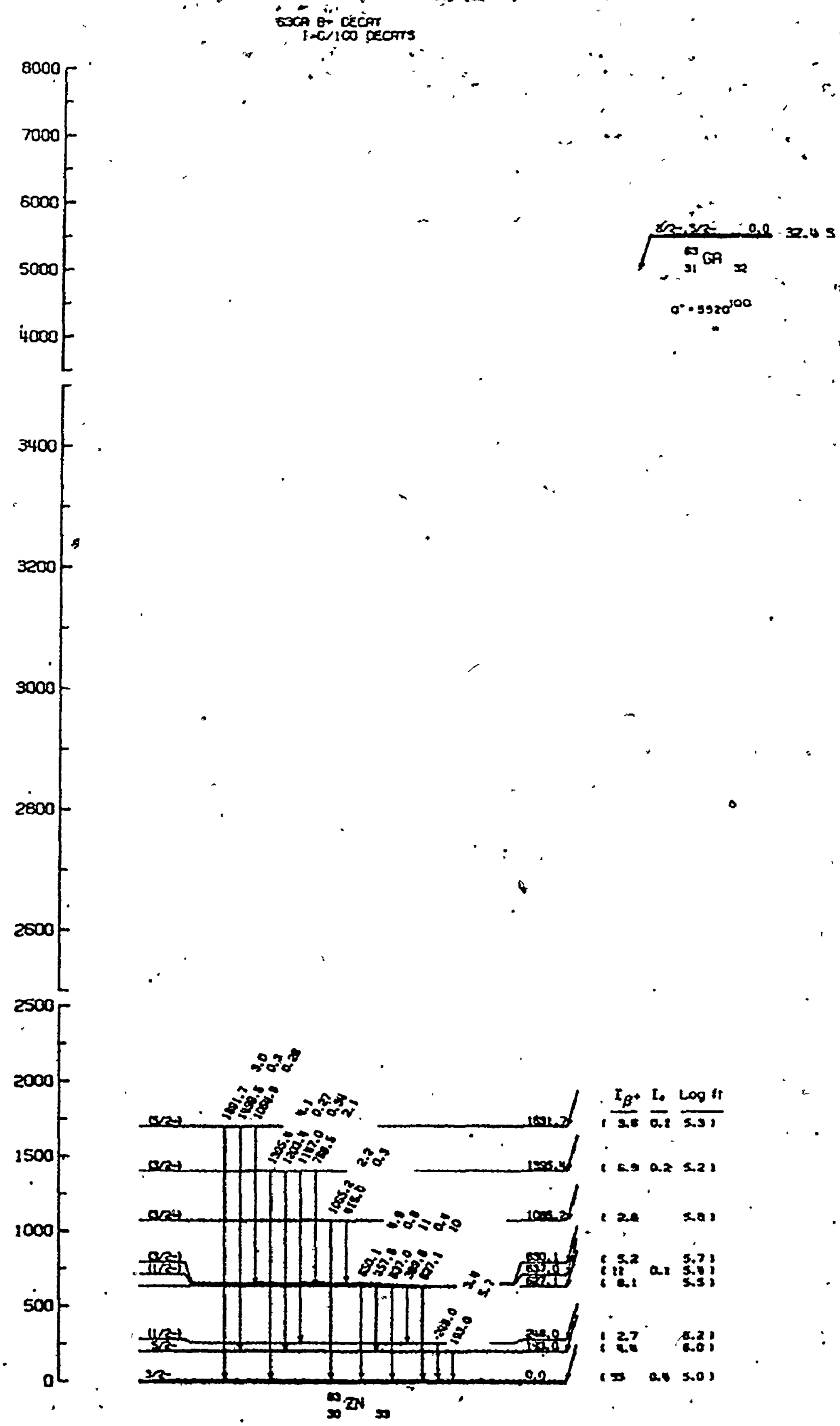
63GA B+ DECAY
I-G/100 DECAYS
8000
7000
6000
5000
4000
3400
3200
3000
2800
2600
2500
2000
1500
1000
500
0
32.4 S
Log ft

fig.2

The $^{60}Ni(\alpha,n\gamma)^{63}Zn$ reaction showing the angular momentum systematics.

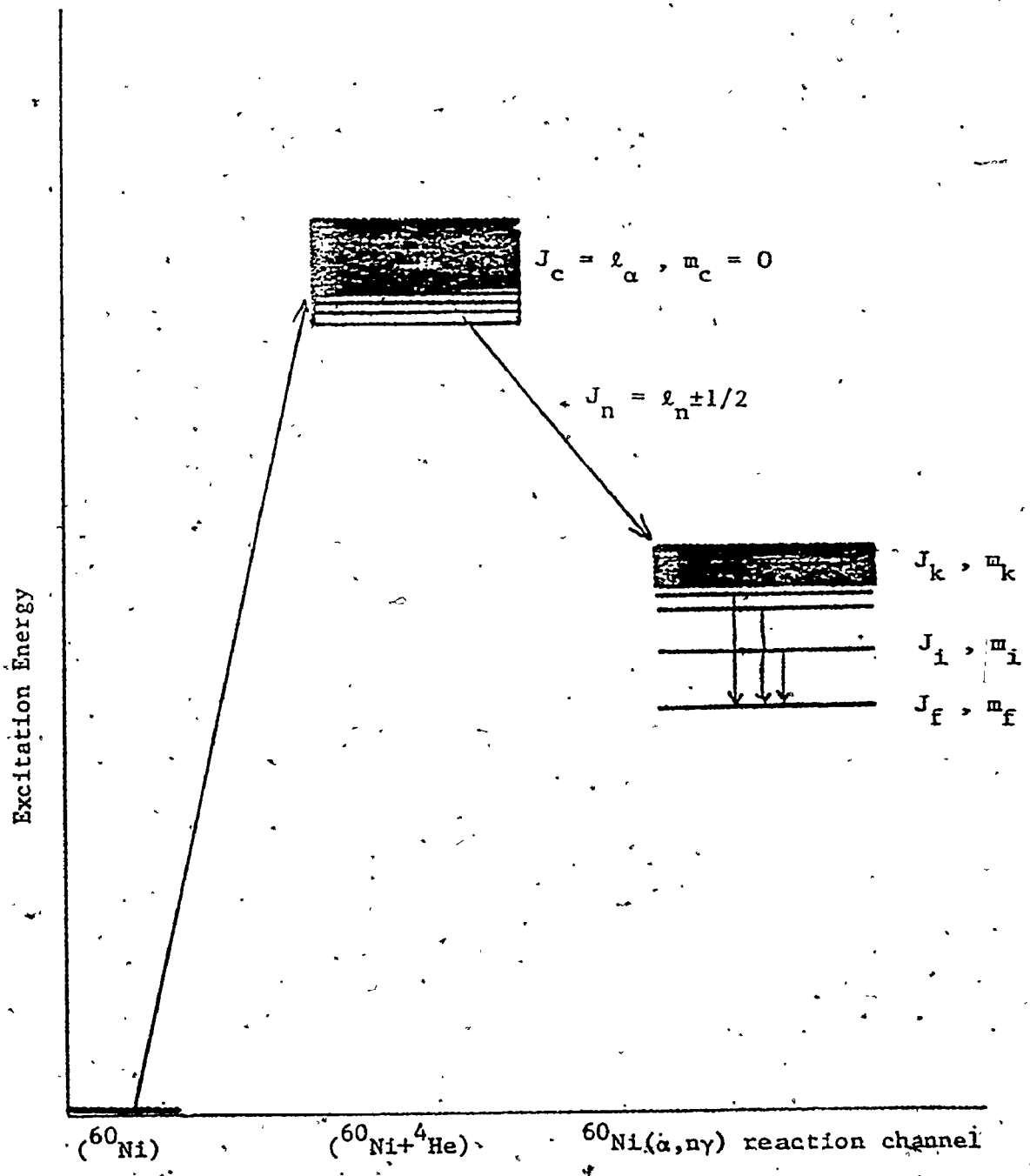

$$J_c = \ell_\alpha \ , \ m_c = 0$$

$$(\ell_\alpha + 1/2) \leq J_k \leq |\ell_\alpha - \ell_n - 1/2| \ , \ m_k = \ell_n \pm 1/2$$

fig.3

The target chamber for the $^{60}Ni(\alpha,n\gamma)^{63}Zn$ experiment.

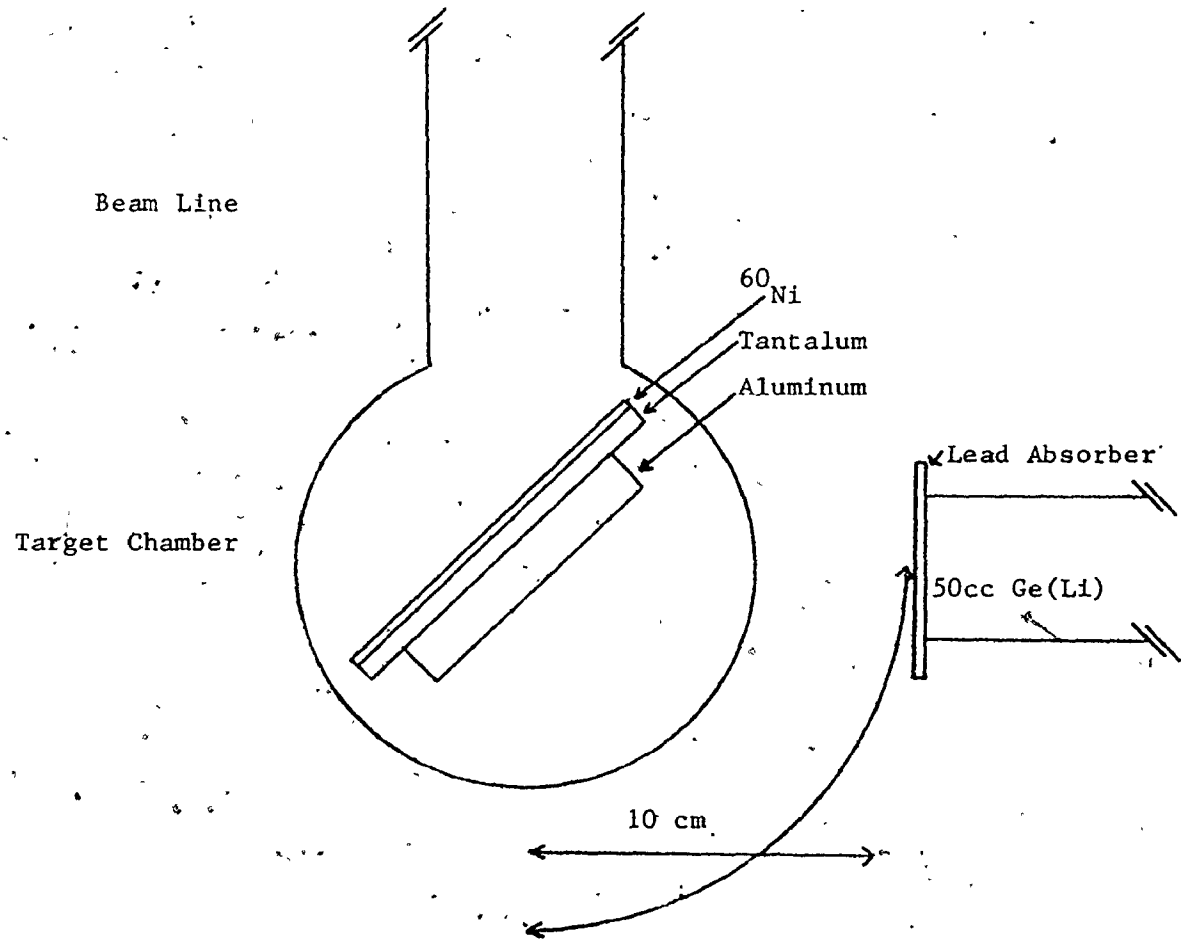
Beam Line
60Ni
Tantalum
Aluminum
Lead Absorber
Target Chamber
50cc Ge(Li)
10 cm

fig.4

γ singles spectrum from $^{60}Ni(\alpha,n\gamma)^{63}Zn$ experiment

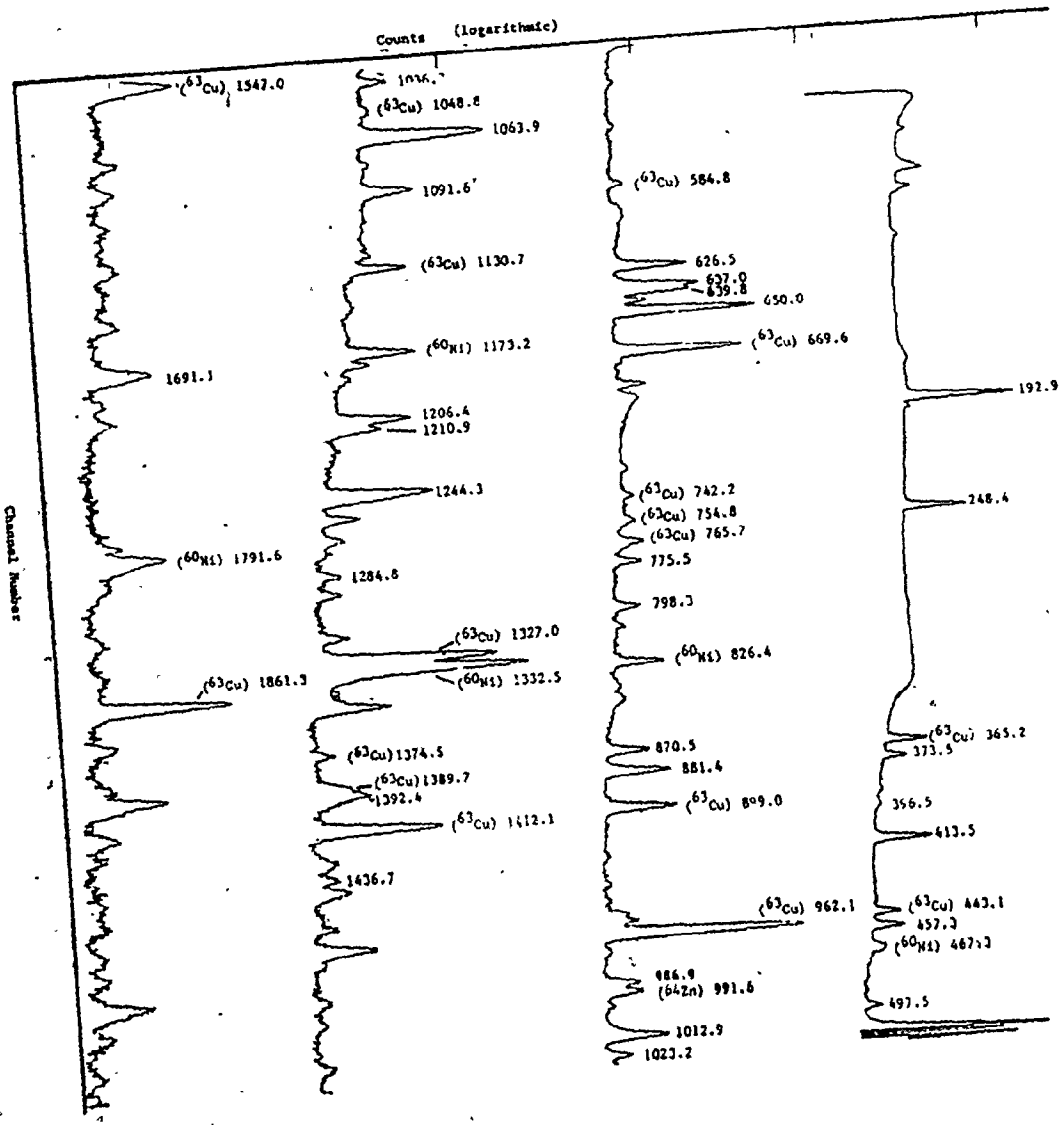
Counts (logarithmic)
Channel Number
(^{63}Cu) 1547.0
1691.1
(^{60}Ni) 1791.6
(^{63}Cu) 1861.3
(^{63}Cu) 1048.8
1063.9
1091.6
(^{63}Cu) 1130.7
(^{60}Ni) 1173.2
1206.4
1210.9
1244.3
1284.8
(^{63}Cu) 1327.0
(^{60}Ni) 1332.5
(^{63}Cu) 1374.5
(^{63}Cu) 1389.7
1392.4
(^{63}Cu) 1412.1
1436.7
(^{63}Cu) 584.8
626.5
637.0
639.8
650.0
(^{63}Cu) 669.6
(^{63}Cu) 742.2
(^{63}Cu) 754.8
(^{63}Cu) 765.7
775.5
798.3
(^{60}Ni) 826.4
870.5
881.4
(^{63}Cu) 909.0
(^{63}Cu) 962.1
986.9
(^{64}Zn) 991.6
1012.9
1023.2
192.9
248.4
(^{63}Cu) 365.2
373.5
386.5
413.5
(^{63}Cu) 443.1
457.3
(^{60}Ni) 467.3
497.5

fig.5

Ge(Li) efficiency curve, obtained using the corrected yields from the competing reaction $^{60}Ni(\alpha,p\gamma)^{63}Cu$. (absorption effects are not included)

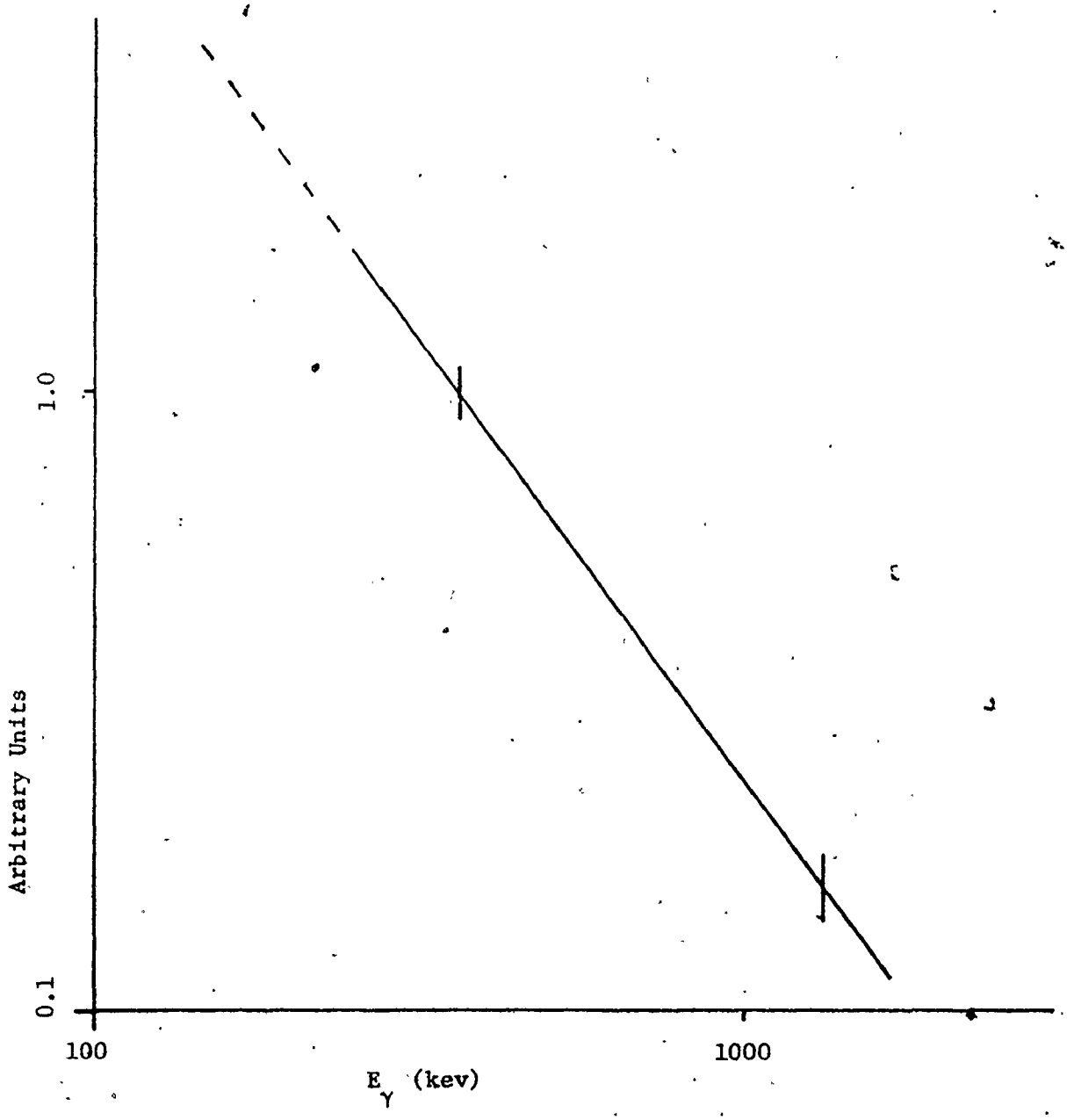
1.0
0.1
Arbitrary Units
100
1000
E_γ (kev)

fig.6

These fits were obtained by varying σ over the range $0.3 \leq \sigma \leq 3.0$. The value $\sigma = 1.0$ was the best fit.

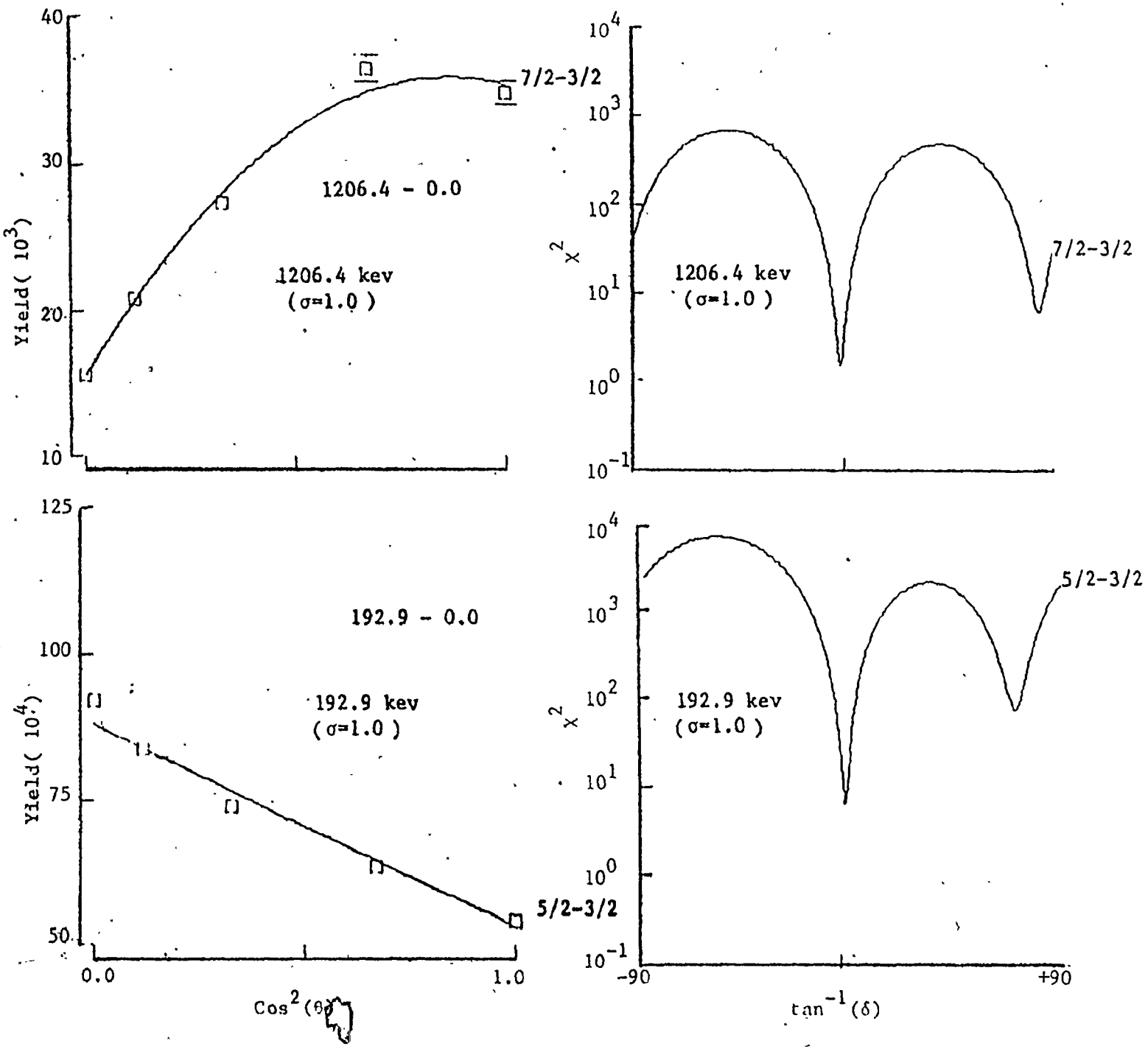
40
30
20
10
Yield(10^3)
7/2-3/2
1206.4 - 0.0
1206.4 kev
(σ=1.0)
10^4
10^3
10^2
10^1
10^0
10^{-1}
χ^2
7/2-3/2
1206.4 kev
(σ=1.0)
125
100
75
50
Yield(10^4)
192.9 - 0.0
192.9 kev
(σ=1.0)
0.0
1.0
$\cos^2(\theta)$
10^4
10^3
10^2
10^1
10^0
10^{-1}
χ^2
5/2-3/2
192.9 kev
(σ=1.0)
5/2-3/2
-90
+90
$\tan^{-1}(\delta)$

fig.7

Schematic for the $\gamma-\gamma$ coincidence experiment

TFA Ortec 454 timing filter amplifier

CFD Ortec 473A constant fraction discriminator

D Ortec 416A gate and delay generator

LA Tennelec TC203 BLR linear amplifier

LGS Ortec 442 linear gate stretcher

TAC Ortec 467 time to pulse height converter/SCA

LS&D Canberra 1455 logic stretcher and delay

ADC Northern NS626 analogue to digital converter

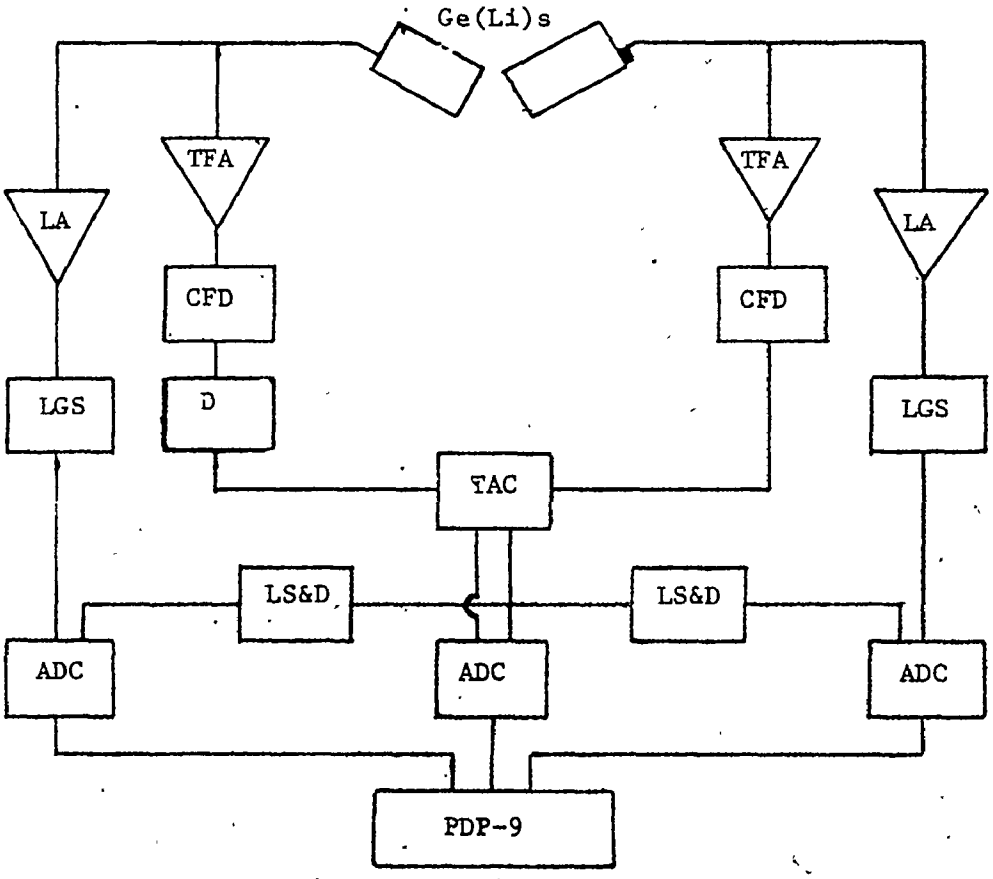
Ge(Li)s
TFA
TFA
LA
LA
CFD
CFD
LGS
D
LGS
TAC
LS&D
LS&D
ADC
ADC
ADC
PDP-9

fig.8

γ-γ coincidence gates

These are representative of the more important transitions in the ^{63}Zn decay scheme.

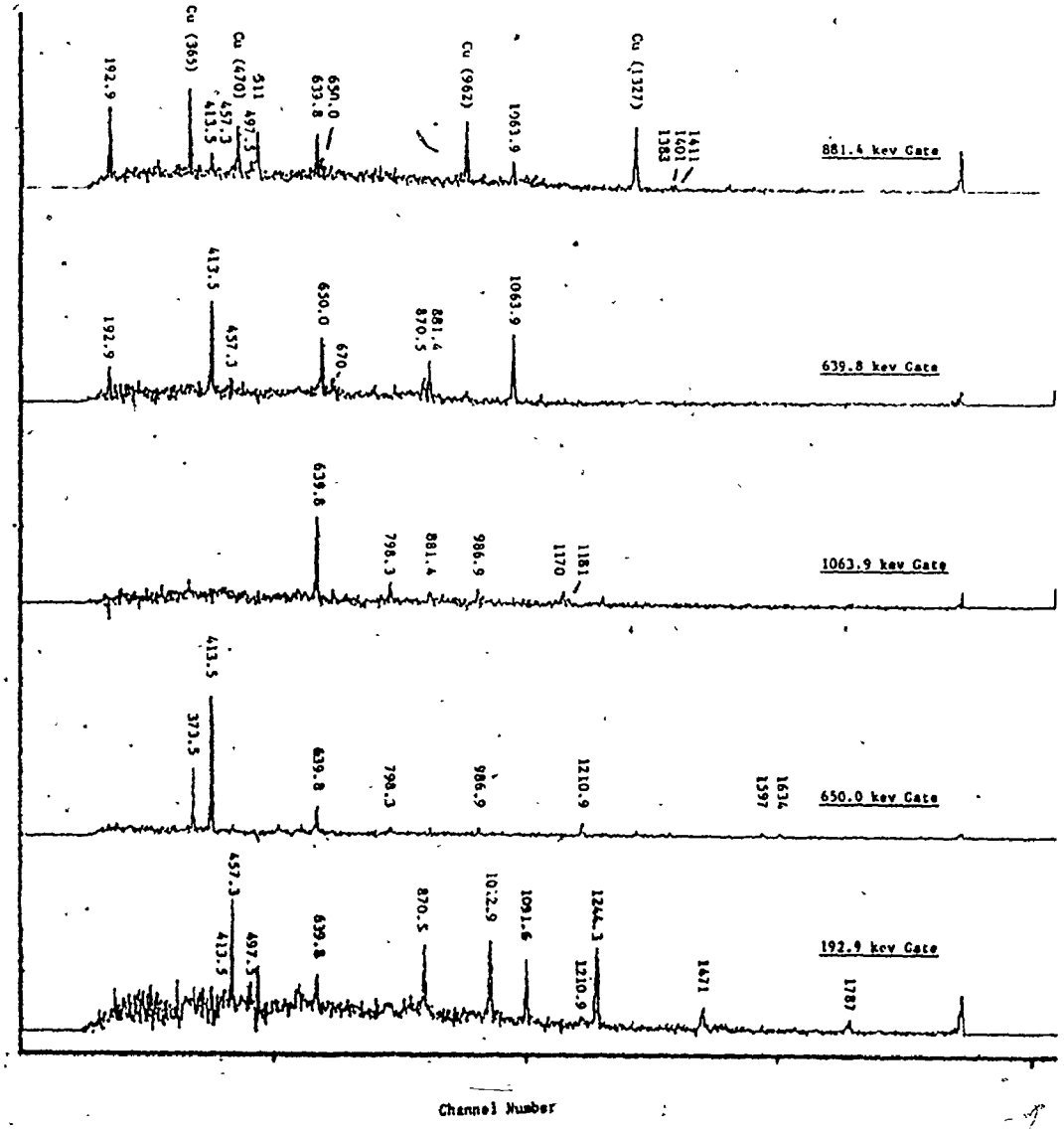
Cu (365)
Cu (470)
511
Cu (962)
Cu (1327)
192.9
413.5
457.3
497.5
650.0
639.8
1063.9
1411
1401
1383
881.4 kev Gate
881.4
870.5
670.
639.8 kev Gate
798.3
986.9
1170
1181
1063.9 kev Gate
373.5
1210.9
1634
1597
650.0 kev Gate
1022.9
1091.6
1244.3
1471
1787
192.9 kev Gate
Counts
Channel Number

fig.9

The ^{63}Zn decay scheme as determined from the $^{60}Ni(\alpha,n\gamma)^{63}Zn$ reaction. Spin assignments are from the γ angular distribution analysis.

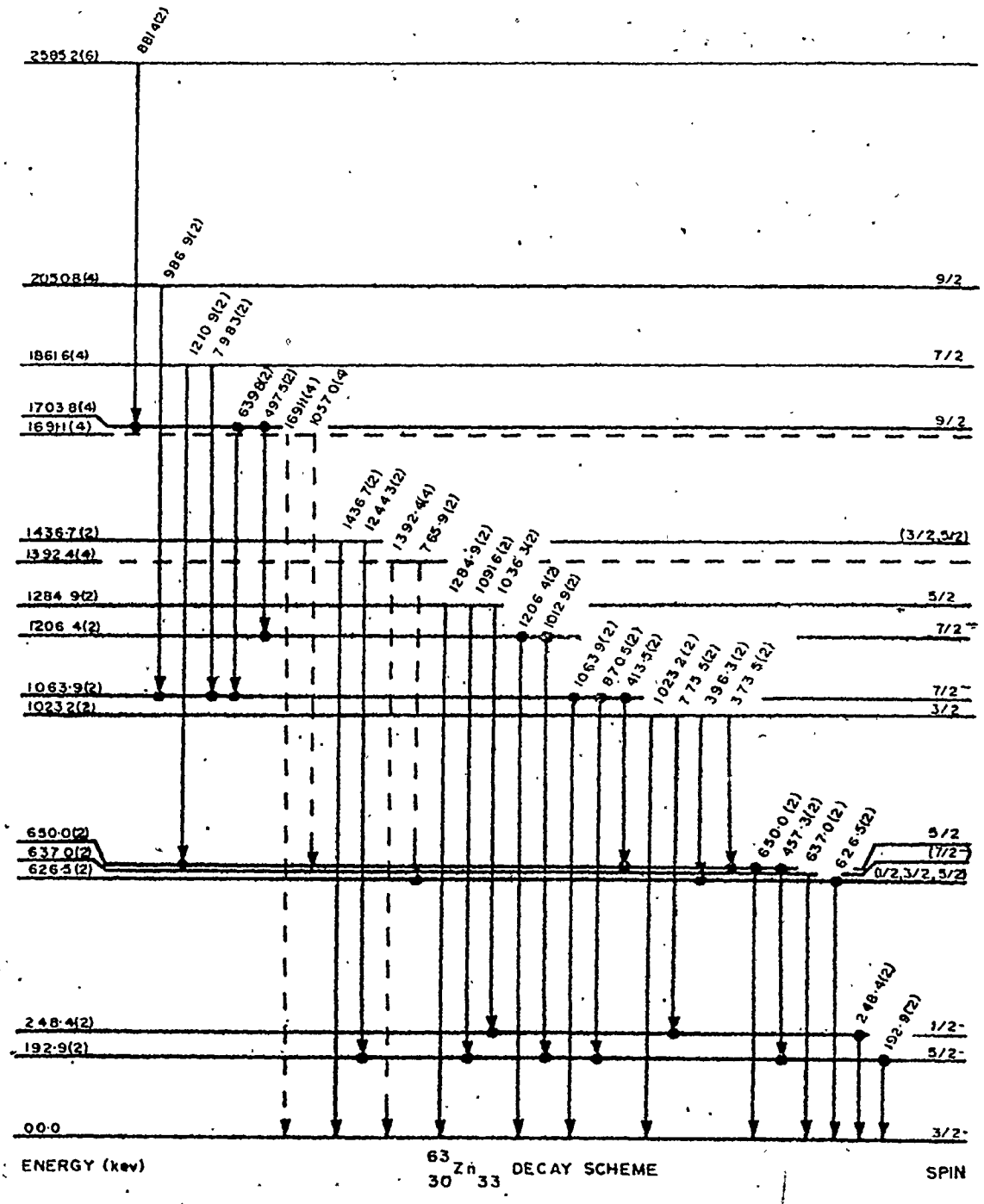
2595.2(6)
881.4(2)
2050.8(4)
986.9(2)
9/2
1861.6(4)
1210.9(2)
798.3(2)
7/2
1703.8(4)
1691.1(4)
639.8(2)
497.5(2)
169.1(4)
1037.0(4)
9/2
1436.7(2)
1392.4(4)
1284.9(2)
1206.4(2)
1012.9(2)
1443.7(2)
1392.4(4)
765.9(2)
1091.6(2)
1036.3(2)
(3/2,5/2)
5/2
7/2
1063.9(2)
1023.2(2)
1063.9(2)
870.5(2)
413.5(2)
1023.2(2)
773.5(2)
396.3(2)
373.5(2)
7/2
3/2
650.0(2)
637.0(2)
626.5(2)
650.0(2)
457.3(2)
637.0(2)
626.5(2)
5/2
(7/2)
(1/2,3/2,5/2)
248.4(2)
192.9(2)
248.4(2)
192.9(2)
1/2-
5/2-
0.0
3/2-
ENERGY (kev)
63 30 Zn 33 DECAY SCHEME
SPIN

fig.10

γ| angular distributions from the $^{60}Ni(\alpha,n\gamma)^{63}Zn$ reaction. These represent the controversial spin assignments.

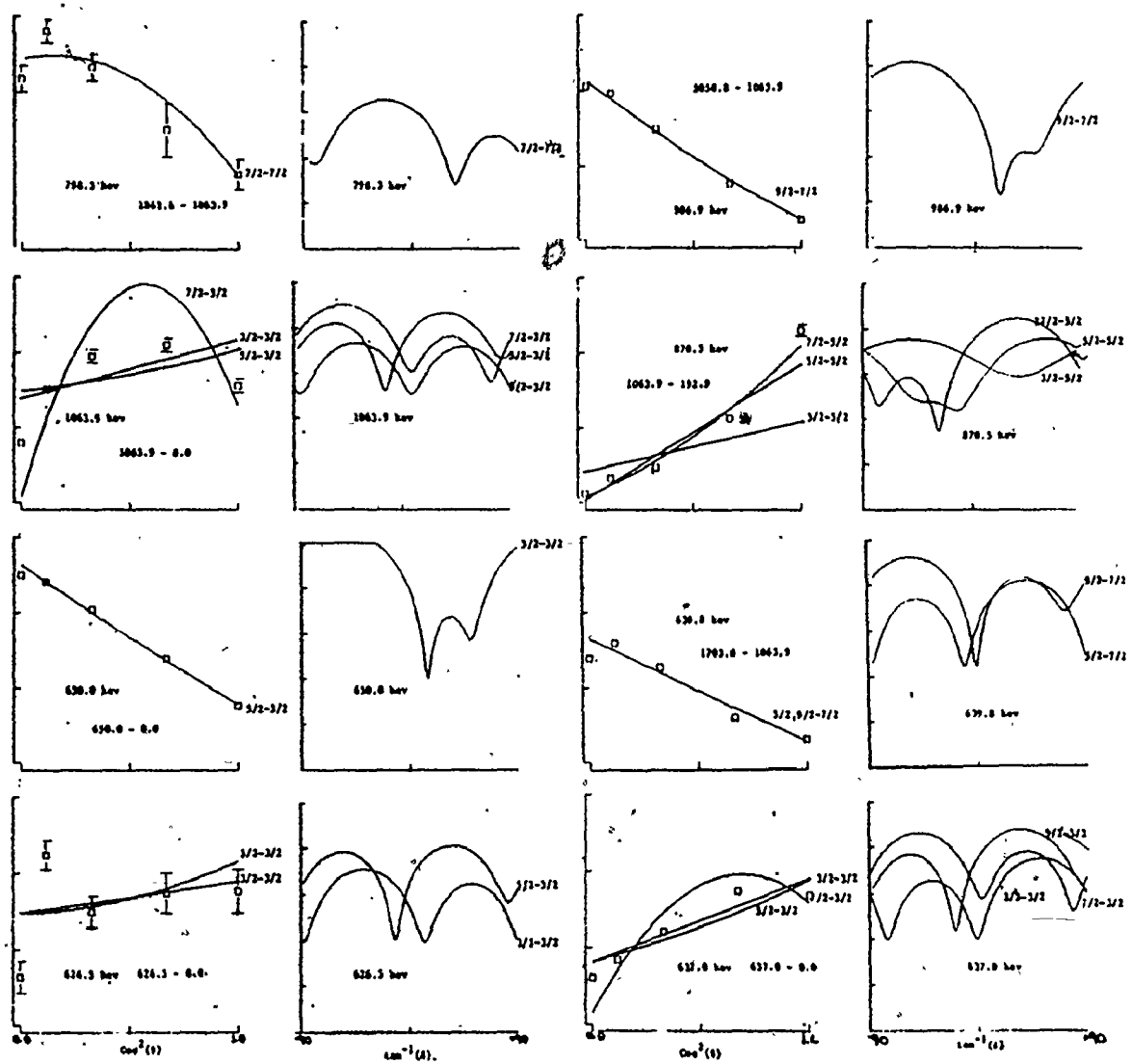
798.3 kev
1063.9 - 1063.9
7/2-7/2
798.3 kev
7/2-7/2
1063.9 - 1063.9
5/2-7/2
906.9 kev
5/2-7/2
906.9 kev
7/2-3/2
3/2-3/2
5/2-3/2
1063.9 kev
1063.9 - 0.0
1063.9 kev
7/2-3/2
5/2-3/2
5/2-3/2
870.5 kev
1063.9 - 193.9
7/2-5/2
5/2-5/2
5/2-5/2
3/2-5/2
5/2-5/2
3/2-5/2
870.5 kev
650.0 kev
650.0 - 0.0
5/2-5/2
650.0 kev
3/2-3/2
639.8 kev
1703.8 - 1063.9
5/2,9/2-7/2
639.8 kev
9/2-7/2
5/2-7/2
626.5 kev
626.5 - 0.0
3/2-3/2
3/2-3/2
626.5 kev
7/2-5/2
3/2-5/2
637.8 kev
637.8 - 0.0
3/2-3/2
3/2-3/2
3/2-3/2
637.8 kev
9/2-3/2
5/2-3/2
7/2-3/2
Cos²(θ)
Sin⁻¹(θ)
Cos²(θ)
Sin⁻¹(θ)

fig,11

Electronic schematic for the $^{64}Zn(p,d)^{63}Zn$ proportional counter experiment.

PA Ortec 109PC pre-amp

LA Tennelec TC203 BLR linear amplifier

TSCA Canberra 1436 timing single channel analyser

C Ortec 418A universal coincidence

LGS Ortec 442 linear gate stretcher

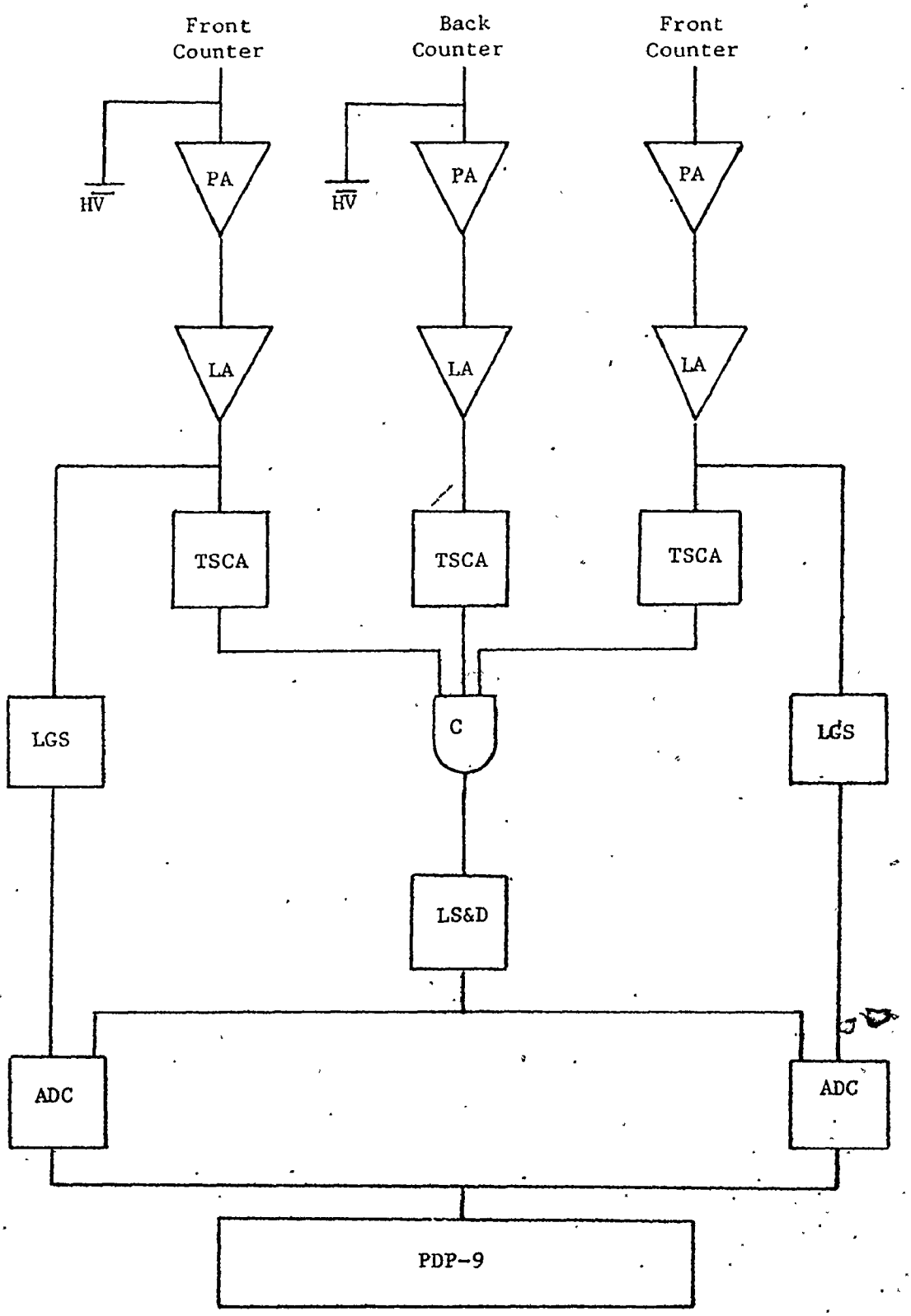
Front Counter
Back Counter
Front Counter
HV
HV
PA
PA
PA
LA
LA
LA
TSCA
TSCA
TSCA
LGS
C
LGS
LS&D
ADC
ADC
PDP-9

fig.12

Energy loss spectrum from the $^{64}Zn(p,d)^{63}Zn$ experiment. Note the ratio of proton to deuteron events.

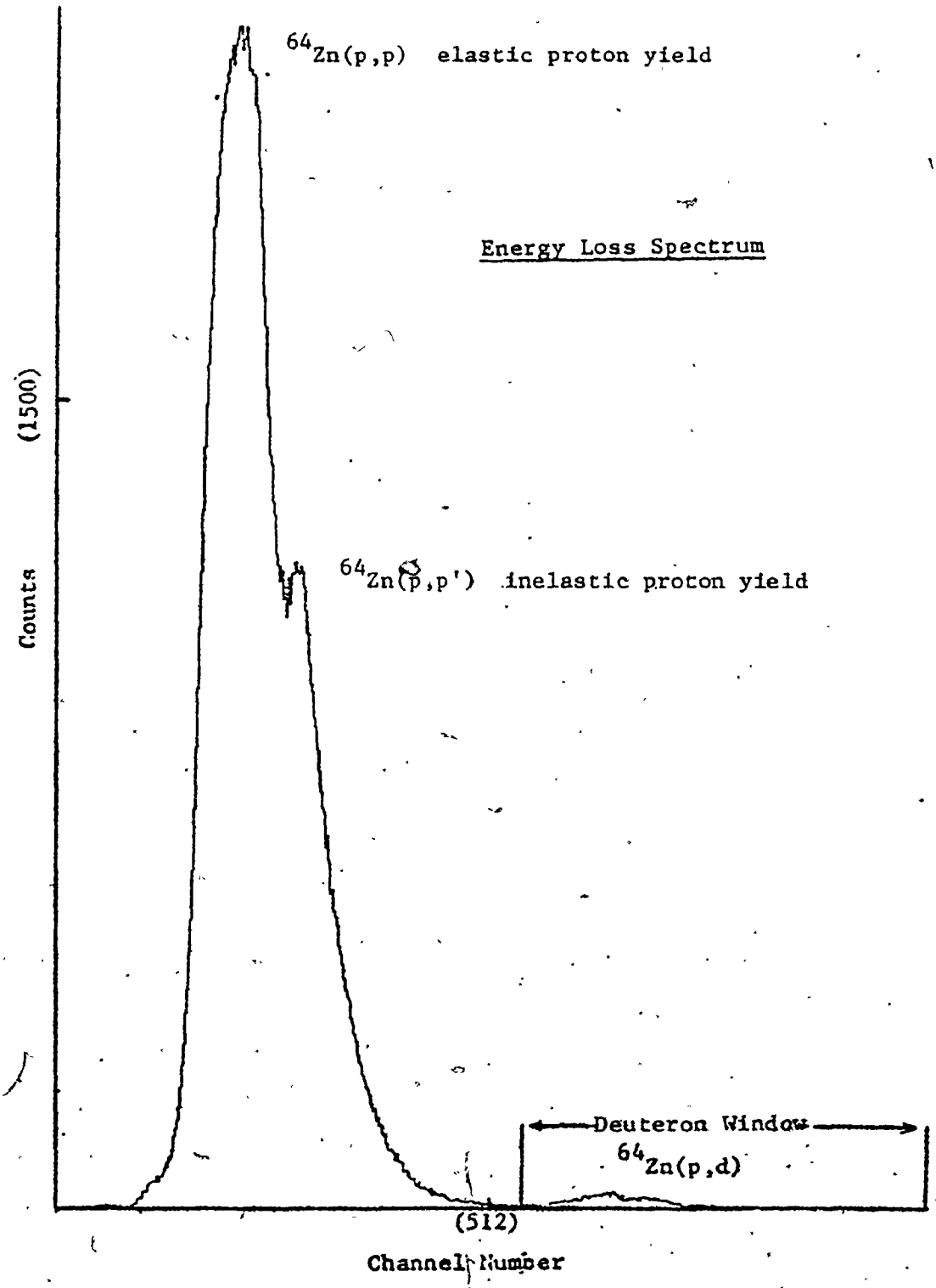
^{64}Zn(p,p) elastic proton yield
Energy Loss Spectrum
(1500)
Counts
^{64}Zn(p,p') inelastic proton yield
Deuteron Window
^{64}Zn(p,d)
(512)
Channel Number

fig.13

The $^{64}Zn(p,d)^{63}Zn$ deuteron position spectrum

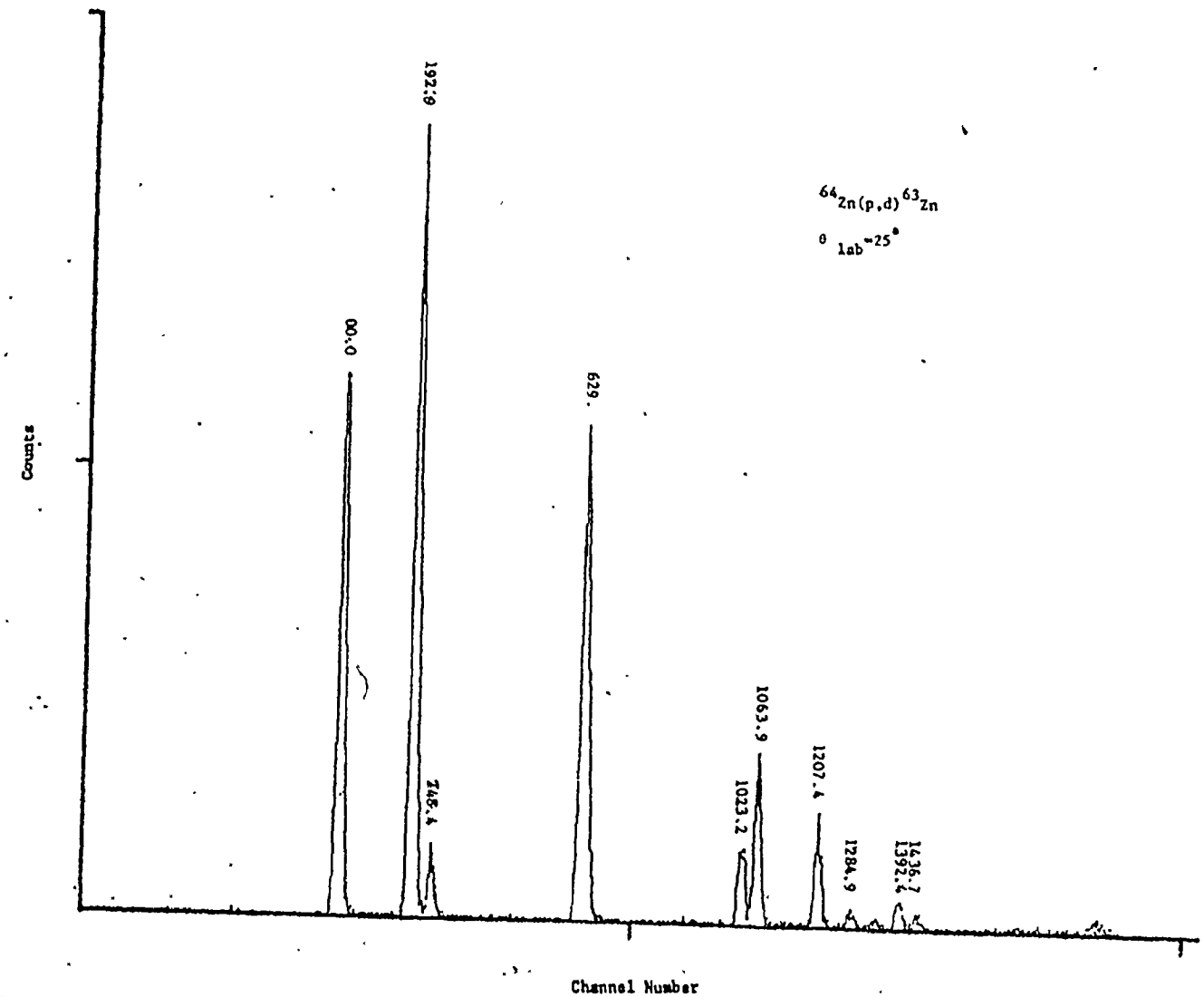
$^{64}Zn(p,d)^{63}Zn$
$\theta_{lab}=25^{\circ}$
Counts
Channel Number
00.0
192.9
629.
746.4
1023.2
1063.9
1207.4
1284.9
1392.4
1636.7

fig.14

DWBA-fitted cross sections using the reaction $^{64}Zn(p,d)^{63}Zn$.

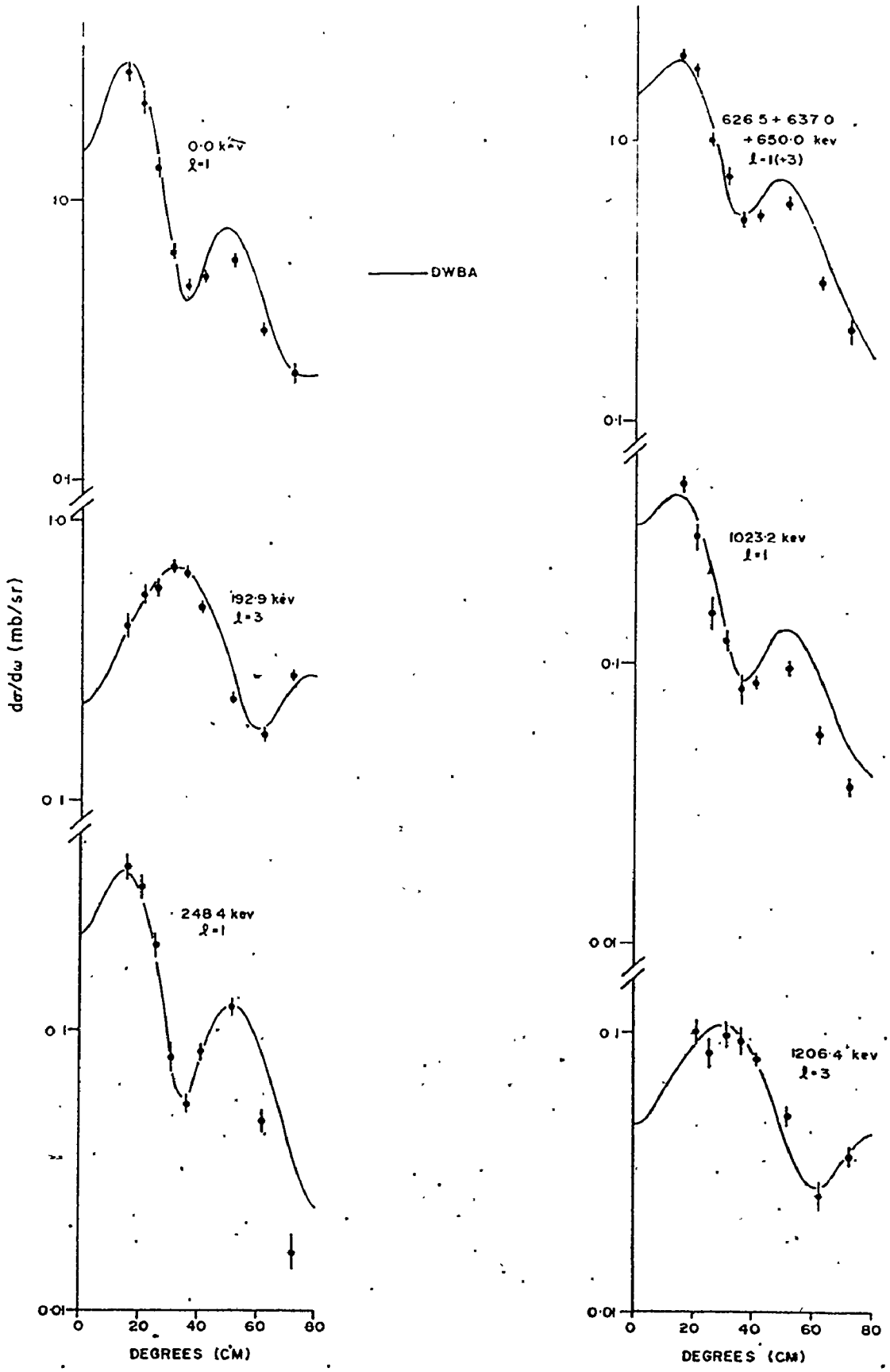
0·0 kev
l=1
192·9 kev
l=3
248·4 kev
l=1
626·5 + 637·0
+650·0 kev
l=1(+3)
1023·2 kev
l=1
1206·4 kev
l=3
DWBA
dσ/dω (mb/sr)
DEGREES (CM)
DEGREES (CM)

fig.15

The 1063.9 kev level differential cross section fitted with an $\ell=1+3$ mixture ,and the un fitted cross sections.

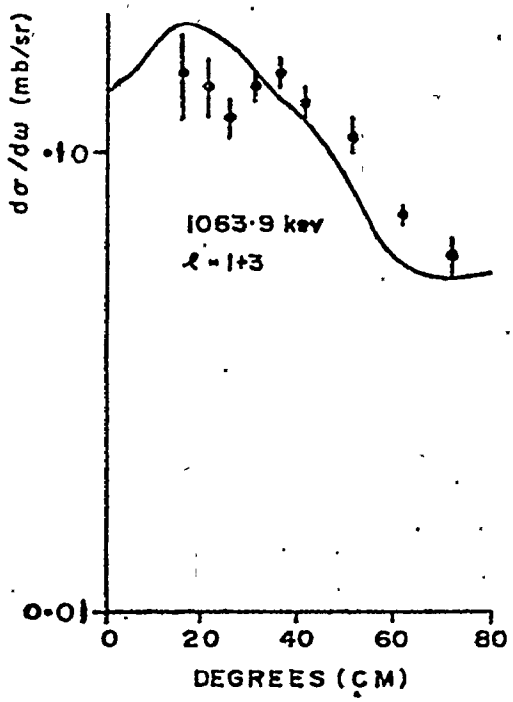
dσ/dω (mb/sr)
·10
0·01
1063·9 kev
ℓ = 1+3
0
20
40
60
80
DEGREES (CM)

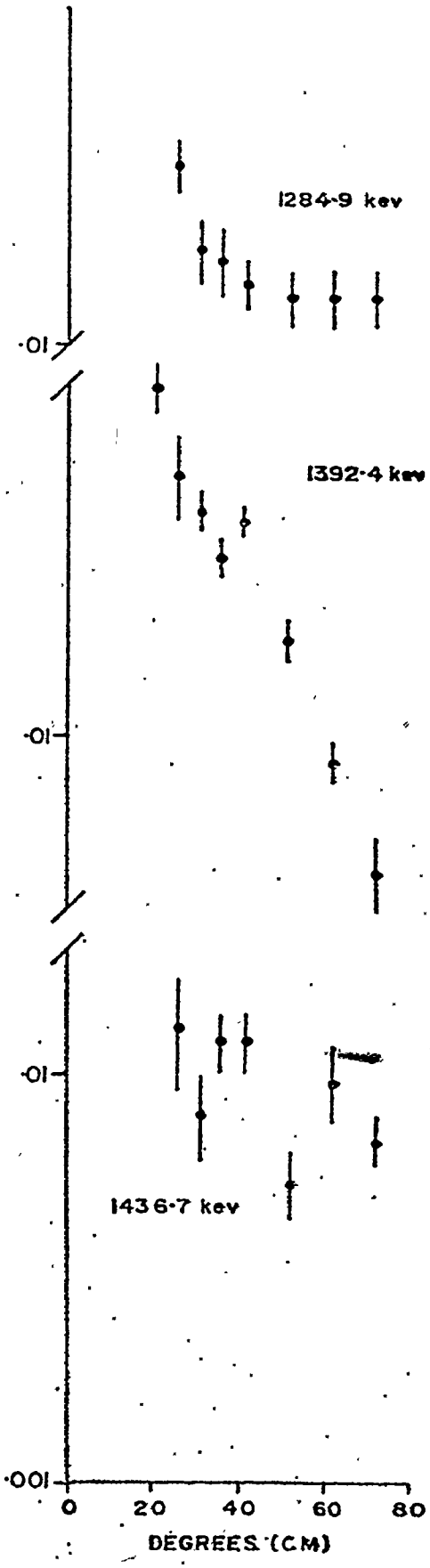
1284·9 kev
·01
1392·4 kev
·01
·01
1436·7 kev
·001
0
20
40
60
80
DEGREES (CM)

fig.16

The 1063.9 kev γ transition from the (α',nγ) experiment assuming a 50% isotropic contribution.

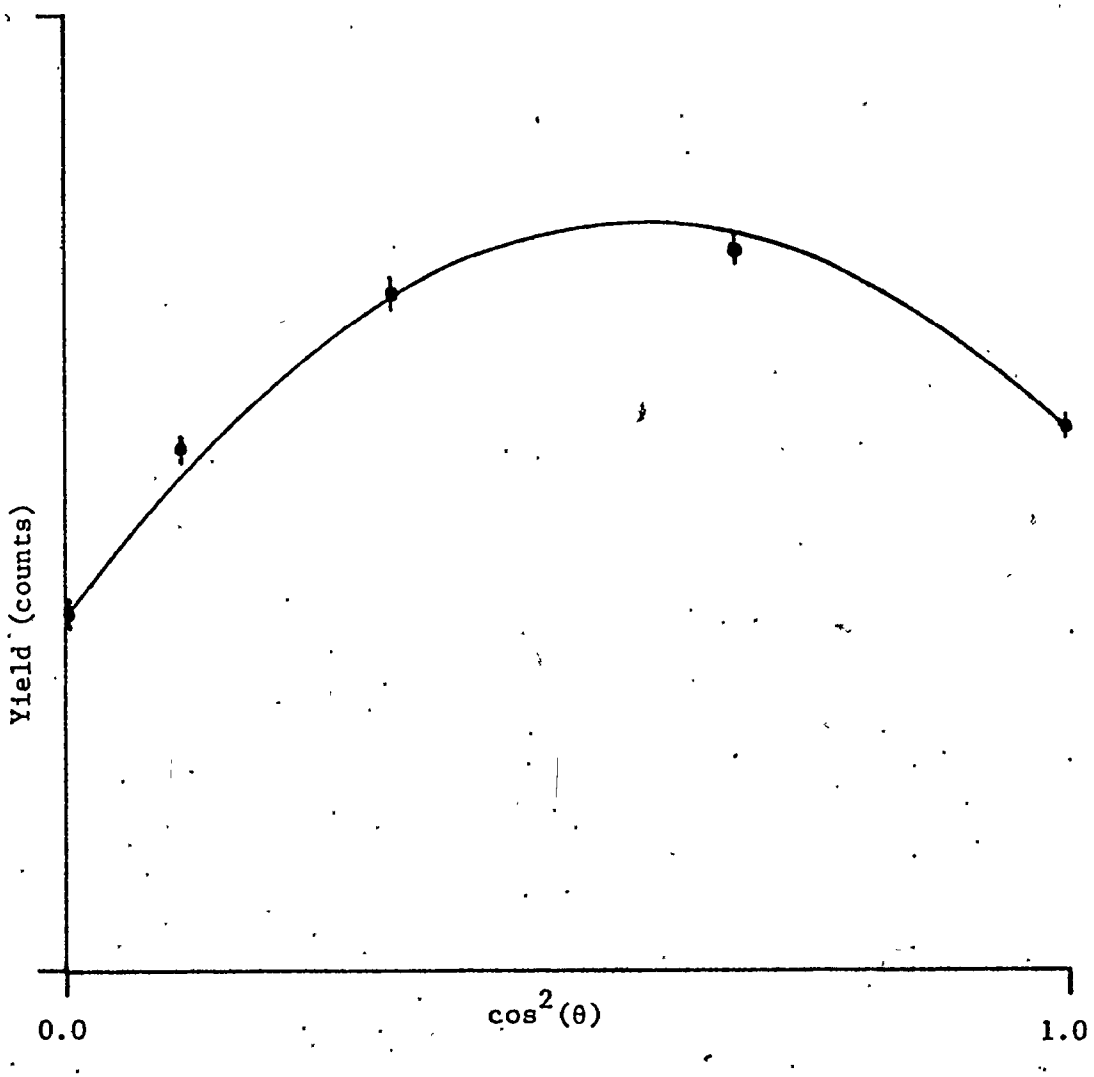
Yield (counts)
0.0
cos^2(θ)
1.0

fig.17

A comparison of the experimental ^{63}Zn level scheme with the theoretical level scheme calculated using the MSDI model

* This doublet was not resolved. One component was assigned a spin and parity $7/2^-$. The other state was tentatively assigned a spin and parity of either $1/2^-$, or $3/2^-$.

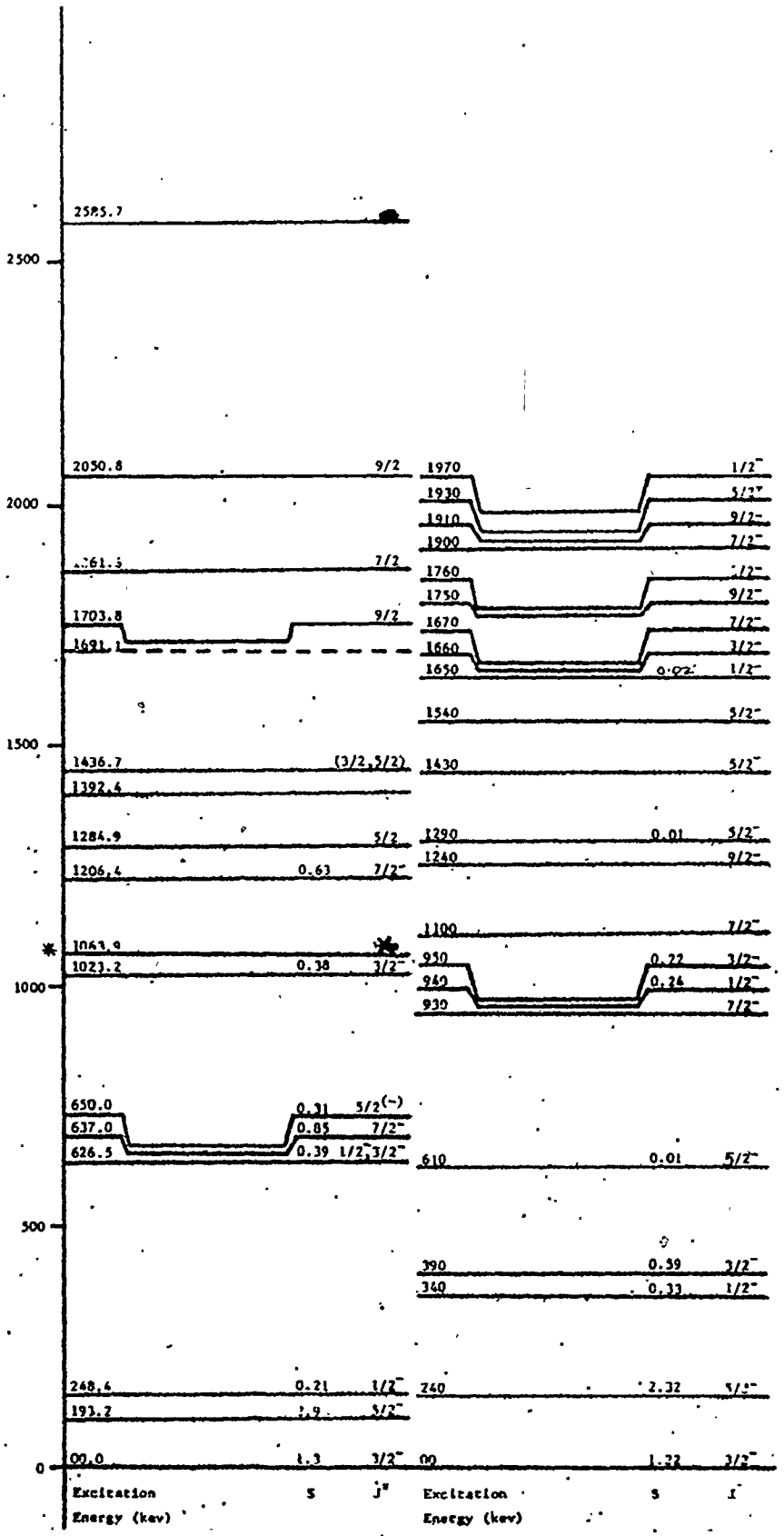
2585.7
2500
2050.8 9/2
2000
1703.8 9/2
1691.1
1500
1436.7 (3/2,5/2)
1392.4
1284.9 5/2
1206.4 0.63 7/2⁻
1063.9
1023.2 0.38 3/2⁻
1000
650.0 0.31 5/2(-)
637.0 0.85 7/2⁻
626.5 0.39 1/2,3/2⁻
500
248.4 0.21 1/2⁻
191.2 5/2⁻
0 00.0 3/2⁻
Excitation Energy (kev)
S
Jπ
Experimental
1970 1/2⁻
1930 5/2⁻
1910 9/2⁻
1900 7/2⁻
1760
1750 9/2⁻
1670 7/2⁻
1660 3/2⁻
1650 0.02 1/2⁻
1540 5/2⁻
1430 5/2⁻
1290 0.01 5/2⁻
1240 9/2⁻
1100 7/2⁻
950 0.22 3/2⁻
940 0.26 1/2⁻
930 7/2⁻
610 0.01 5/2⁻
390 0.39 3/2⁻
340 0.33 1/2⁻
240 2.32
00 1.22 3/2⁻
Excitation Energy (kev)
S
Jπ
NSDI

table 1

The γ-γ coincidence matrix

Peak Energy (kev) \ Gate Energy (kev)	193	248	373	413	457	626	636	640	650	775	798	870	881	987	1014	1063	1093	1210	1244
193			x	x	x			x			x	x	x		x		x	x	x
248										x									
373					x				x										
396						x													
413	x				x		x	x	x		x		x	x					
457	x		x	x				x			x		x					x	
497	x												x		x				
626																			
636																			
640	x			x	x				x			x	x			x			
650			x	x				x			x		x	x				x	
775		x																	
797				x					x							x			
870	x							x											
881								x	x							x			
987				x					x							x			
1012	x																		
1023																			
1036		x																	
1063								x			x		x	x					
1091	x																		
1206																			
1210	x				x				x										
1244	x																		
1284																			
1436																			
Not Placed	1471,1782			955			1057	670	1597,1634				1388,1401, 1411			1170,1181	1090		

$^{60}Ni(\alpha,n\gamma)^{63}Zn$, E_α = 12.0 Mev table 2

γ transition characteristics

Energy (kev)	Intensity	Classification	Experimental A_2	Experimental A_4	Spin Assignments	χ^2	Calculated A_2	Calculated A_4	$\tan^{-1}(\delta)$ (degrees)
192.9(2)	1.00(8)	193-0	-.25(1)	.04(1)	5/2-3/2	0.7	-.23	0.00	-2
248.4(2)	.25(2)	248-0	(isotropic)		1/2-3/2	-	-	-	-
373.5(2)	.049(5)	1023-650	.12(2)	.00(3)	3/2,5/2, 7/2-5/2	0.9,0.8, 0.8	.12,.12, .13	0.0,.01, .02	21,14, -33
396.3(2)	.008(1)	1023-626	-	-	-	-	-	-	-
413.5(2)	-	1063-650	-.40(2)	-.05(2)	5/2,7/2 -5/2	4,5	-.36,-.42	-.07,0.00	60,4
457.3(2)	.059(5)	650-193	.33(2)	-.04(2)	5/2-5/2	2.0	.32	0.00	0
497.5(2)	.024(3)	1703-1206	-.28(5)	.05(5)	5/2,9/2 -7/2	0.6,0.8	-.27,-.28	0.0,0.0	(-90,-8), -1
626.5(2)	.43(3)	626-0	.03(1)	-.03(2)	1/2,3/2, 7/2-3/2	-	-	-	-
637.0(2)	.24(2)	637-0	.20(1)	-.09(2)	3/2,5/2, 7/2-3/2				
639.8(2)	.15(1)	1703-1063	-.28(1)	-.02(2)	5/2,9/2 -7/2	16,16	-.29,-.30	0.0,0.0	-10,0
650.0(2)	.48(4)	650-0	-.58(1)	-.03(1)	5/2-3/2	10	-.62	.01	16
775.5(2)	.031(3)	1023-248	-.32(4)	-.02(4)	3/2-1/2	5.5	-.34	0.0	(9,31)
798.3(2)	.040(4)	1861-1063	-.16(4)	-.11(4)	7/2-7/2	2.8	-.16	-.1	38
870.5(2)	.085(8)	1063-193	.46(2)	.15(2)	7/2-5/2	6.0	.47	.07	-27
881.4(2)	-	2585-1703	-	-	-	-	-	-	-
986.9(2)	.043(4)	2050-1063	-.87(4)	.04(4)	9/2-7/2	1.2	-.87	.05	21

table 2 (continued)

Energy (kev)	Intensity	Classification	Experimental A_2	Experimental A_4	Spin Assignments	χ^2	Calculated A_2	Calculated A_4	$\tan^{-1}(\delta)$ (degrees)
1012.9(2)	.13(1)	1206-192	.35(2)	.20(2)	7/2-5/2	12	.33	.34	(-80,-23)
1023.2(2)	.037(4)	1023-0	.39(4)	.03(4)	3/2,5/2 -3/2	2.3,2.0	.39,.38	0.0,.04	(-58,-19),-22
1036.3(2)	.045(5)	1284-248	.45(3)	.28(4)	5/2-1/2	3	.39	.20	0
1063.9(2)	.62(5)	1063-0	.11(1)	-.14(1)	3/2,5/2, 7/2-3/2	-	-	-	-
1091.6(2)	.12(1)	1284-193	.03(2)	-.05(2)	5/2,7/2 -5/2				
1206.4(2)	.16(1)	1206-0	.44(2)	-.18(2)	7/2-3/2	1.5	.44	-.17	-1
1210.9(2)	.082(8)	1861-650	.52(2)	-.22(3)	5/2,7/2 -5/2	30,60	.06,.07	.48,.45	-45,-26
1244.3(2)	-	1436-193	.47(1)	-.21(2)	9/2-5/2	3	.44	-.17	0
1284.8(2)	.011(2)	1284-0	-1.2(2)	-.2(2)	5/2-3/2	6	-.82	.07	37
1436.7(2)	.011(3)	1436-0	-.3(1)	0.0(1)	3/2,5/2 -3/2	.5,.4	-.27,-.31	0.0,0.0	50,1

table 3

Optical Model Parameters

particle	V_R (Mev)	r_R (fm)	a_R (fm)	W_v (Mev)	r_v (fm)	a_v (fm)	W_s (Mev)	r_s (fm)	a_s (fm)	V_{so} (Mev)	r_{so} (fm)	a_{so} (fm)	non-local correction parameter
p	52.4	1.17	0.75	1.3	1.32	0.54	7.9	1.32	0.54	12.4	1.01	0.75	0.85
d	-107.7	1.05	0.86	-	-	-	13.8	1.43	0.70	7.0	0.75	0.50	0.54
n	*	1.17	0.75	-	-	-	-	-	-	$0.28V_R$	1.17	0.75	0.85

the coulomb potential is due to a uniformly charged sphere of radius $1.3A^{(1/3)}$ and charge $Z_A e$

the finite range correction parameter = 0.621

no radial cut-off was used

* adjusted to reproduce separation energy

table 4

ℓ values and spectroscopic values

	Excitation Energy (kev)	ℓ	S (±20%)
	000.0	1	1.3
	192.9	3	2.9
	248.4	1	0.21
	627.	1	0.39
Unresolved	637.	(1,3)	(<0.1, <0.85)
	650.	(1,3)	(<0.04, <0.31)
	1023.2	1	0.38
	1063.9	(1+3)	0.21 ,0.37
	1206.4	3	0.63
	1284.8	-	-
	1392.4	-	-
	1436.7	-	-

References

Austern,N. 1970. "Direct Nuclear Reaction Theories" Wiley Interscience.

Becchetti,F.D. and Greenlees,G.W. 1969. Phys. Rev. 182, 1190.

Betigeri,M.G., Duhm,H.H., Santo,R., Stock,R. and Bock,R. 1967. Nucl. Phys. A100, 416.

Birstein,L., Drory,Ch., Jaffe,A.A. and Zioni,Y. 1967. Nucl. Phys. A97, 203.

Birstein,L., Chechik,R., Drory,Ch., Freidman,E., Jaffe,A.A. and Wolf,A. 1968. Nucl. Phys. A113, 193.

Brandan,M.E. and Haeberli,W. 1977. Nucl. Phys. A287, 205.

Davisson,C.M. and Evans,R.D. 1952. Rev. Mod. Phys. 24, 79

Geisler,G.C. 1971 Ph.D. Thesis. Mich. State. Univ.; Diss. Abstr. Int. 323, 5091 (1972)

Glaudemans,P.W.M., Brussard,P.J. and Wildenthal,B.H. 1967. Nucl. Phys. A102, 593.

Johnson,R.R. and Jones,G.D. 1968. Nucl. Phys. A122, 657.

Klaase,A.A. and Goudsmit,P.F.A. 1974. Z. Physik. 266 , 75.

Kunz,P.D. 1974. Computer Code DWUCK, Univ. Colorado.

McIntyre,L.C. 1966. Phys. Rev. 152, 152.

Nir,D. and Cameron,J.A. 1977. Can. J. Phys. 55, 531.

Rose, H.J. and Brink,D.M. 1967. Rev. Mod. Phys. 39, 306.

Sawa,Z.P., Nilsson,A. and Sztarkar,J. 1971: Ann. Rept., Reseach Inst. Stockholm, 103.

Sawa,Z.P. 1973 Ph.D. Thesis, Research Inst. Phys., Stockholm.

Spencer,J.E. and Enge,H.A. 1967 Nucl. Instr. and Meth. 49, 181.

Tanaka,S.,Stelson,P.H., Bass,W.T. and Lin,J. 1970 Phys. Rev. C2, 160.

van Heinen,J.F.A., Ching,W. and Wildenthal,B.H. 1976 Nucl. Phys. A269,159